

Correlations, soliton modes, and non-Hermitian linear mode transmutation in the 1D noisy Burgers equation

Hans C. Fogedby

Institute of Physics and Astronomy,

University of Aarhus,

DK-8000, Aarhus C, Denmark

and

NORDITA, Blegdamsvej 17,

DK-2100, Copenhagen, Denmark

(Dated: March 22, 2024)

Abstract

Using the previously developed canonical phase space approach applied to the noisy Burgers equation in one dimension, we discuss in detail the growth morphology in terms of nonlinear soliton modes and superimposed linear modes. We moreover analyze the non-Hermitian character of the linear mode spectrum and the associated dynamical pinning and mode transmutation from diffusive to propagating behavior induced by the solitons. We discuss the anomalous diffusion of growth modes, switching and pathways, correlations in the multi-soliton sector, and in detail the correlations and scaling properties in the two-soliton sector.

PACS numbers: 05.10.Gg, 05.45.-a, 64.60.Ht, 05.45.Yv

Electronic address: fogedby@phys.au.dk

I. INTRODUCTION

This is the fourth of a series of papers on the one dimensional noisy Burgers equation for the slope field of a growing interface. In paper I [1] we discussed as a prelude the noiseless Burgers equation [2, 3] in terms of its nonlinear soliton or shock wave excitations and performed a linear stability analysis of the superimposed dispersive mode spectrum. This analysis provided a heuristic picture of the damped transient pattern formation. As a continuation of previous work on the continuum limit of a spin representation of a solid-on-solid model for a growing interface [4], we applied in paper II [5] the Martin-Siggia-Rose formalism [6] in its path integral formulation [7, 8, 9] to the noisy Burgers equation [10, 11] and discussed in the weak noise limit the growth morphology and scaling properties in terms of nonlinear soliton excitations with superimposed linear dispersive modes. In paper III [12] we pursued a canonical phase space approach based on the weak noise saddle point approximation to the Martin-Siggia-Rose functional or, alternatively, the Freidlin-Wentzel symplectic approach to the Fokker-Planck equation [13, 14]. This method provides a dynamical system theory point of view to weak-noise stochastic processes and yields direct access to the probability distributions for the noisy Burgers equation; brief accounts of paper II and III appeared in [15] and [16].

Far from equilibrium phenomena are common, including turbulence, interface and growth problems, chemical reactions, and a host of other phenomena bordering on biology, sociology and economics. Unlike equilibrium phenomena the nonequilibrium cases are not very well understood and constitute a major challenge in modern statistical physics. Here the Burgers equation provides in many respects the simplest continuum description of a nonlinear initial value problem in the noiseless case and an open driven nonlinear system in the noisy case, exhibiting scaling and pattern formation.

The noisy Burgers equation for the local slope $u(x;t)$ of a growing interface analyzed in papers II and III has the form

$$\frac{\partial}{\partial t} u + \frac{1}{2} u^2 = \nu \frac{\partial^2 u}{\partial x^2} + \eta(x,t); \quad (1.1)$$

here expressed as manifestly invariant under the slope-dependent nonlinear Galilei transformation

$$x \rightarrow x + u_0 t; \quad (1.2)$$

$$u_t = -u + u_0; \quad (1.3)$$

and is equivalent to the much studied Kardar-Parisi-Zhang (KPZ) equation [17, 18] for the height $h(x;t)$, $u = r h$ (in a co-moving frame),

$$\frac{\partial h}{\partial t} = -r^2 h + \frac{1}{2} (r h)^2 + \zeta; \quad (1.4)$$

The growth equations (1.1) and (1.4) are driven by short-range correlated Gaussian white noise determined by the correlation function

$$\langle \zeta_i(xt) \zeta_j(x't') \rangle = \delta(x-x') \delta(t-t'); \quad (1.5)$$

characterized by the noise strength ζ . In Eqs. (1.1) and (1.4) the damping constant or viscosity γ measures the strength of the linear damping term, whereas α control the nonlinear growth or mode coupling term.

From the analysis in papers II and III it follows that the stochastic nonequilibrium problem determined by Eqs. (1.1) and (1.5) in the singular weak noise limit $\zeta \rightarrow 0$ can be replaced by two coupled deterministic Galilean invariant mean field equations coupling the slope field u to the canonically conjugate noise field p

$$\frac{\partial}{\partial t} u + r u^2 = -r^2 u - r^2 p; \quad (1.6)$$

$$\frac{\partial}{\partial t} p + r p^2 = -r^2 p; \quad (1.7)$$

In the path integral analysis in paper II Eqs. (1.6 - 1.7) are saddle point equations for the extremal path in the classical limit $\zeta \rightarrow 0$; in the canonical phase space approach in paper III they are classical canonical field equations determining orbits in an associated phase space. This doubling of dynamical variables in the deterministic description was also encountered in the spin model discussed in [4]. The noise variable ζ in Eq. (1.1) emerges as the canonically conjugate momentum variable p coupling to u .

As discussed in papers II and III, see also [4], the field equations (1.6) and (1.7) in addition to linear dispersive modes also support two distinct soliton modes or domain walls, in the static case of the kink-like form

$$u_s(x) = u \tanh k_s (x - x_0); \quad k_s = u/2; \quad (1.8)$$

Here k_s sets the inverse length scale, $\epsilon = \pm 1$ is a parity index and the soliton is centered at x_0 . For $\epsilon = +1$ we have the right hand soliton which is also a solution of the noiseless

Burgers equation for $\epsilon = 0$ in Eq. (1.1) or for $p = 0$ in Eq. (1.6). For $\epsilon = 1$ we obtain the noise-induced left hand soliton, a new solution of the coupled equations. The associated noise field is $p_s = 0$ for the noiseless $\epsilon = +1$ soliton; for the noisy soliton for $\epsilon = 1$ we have

$$p_s = 2 u \tanh k_s x; \quad (1.9)$$

modulus a constant.

In the noiseless Burgers equation the transient pattern formation is described by Galilee-boosted right hand solitons connected by ramp solutions with superimposed damped linear modes [1, 19, 20, 21]. In the noiseless KPZ equation for the height h this pattern corresponds to smoothed downward cusps connected by parabolic segments with superimposed linear modes [18, 22]. However, in the noisy case the doubling of soliton solutions alters the morphology completely. Here the amplitude-matched Galilee-boosted right and left hand solitons provide a many body description of a stationary growing interface. On the soliton gas is superimposed a gas of linear modes which in the linear Edwards-Wilkinson case [23] for $\epsilon = 0$ becomes the diffusive modes of the noise-driven diffusion equation.

The canonical phase space approach expounded in paper III moreover provides a deterministic dynamical system theory description of a growing interface. With an orbit in canonical phase space from an initial configuration u^i to a final configuration u^f traversed in time T , determined as a specific initial-final value solution of the field equations (1.6) and (1.7), we thus associate the action S

$$S(u^f; u^i; T) = \int_{u^i, 0}^{u^f, T} dt dx \left(p \frac{\partial u}{\partial t} - H \right); \quad (1.10)$$

More explicitly, the transition probability from an initial configuration u^i to a final configuration u^f in time T is determined by

$$P(u^f; u^i; T) = (T)^{-1} \exp \left(-\frac{1}{T} S(u^f; u^i; T) \right); \quad (1.11)$$

$$(T) = \int_{u^i}^{u^f} du^f \exp \left(-\frac{1}{T} S(u^f; u^i; T) \right); \quad (1.12)$$

where we have introduced the dynamical partition function (T) , arising from the normalization condition $\int_{u^i}^{u^f} du^f P(u^f; u^i; T) = 1$. Likewise, the stationary distribution is associated with an infinite-time orbit from u^i to u^f and is given by

$$P_{st}(u^f) = \lim_{T \rightarrow \infty} P(u^f; u^i; T); \quad (1.13)$$

and for example the slope correlation (the second moment of P) in the stationary regime by the expression

$$\langle u^i u^i(\mathbf{x}; T) \rangle = \int d\mathbf{u}^i d\mathbf{u}^f u^f(\mathbf{x}) u^i(0) P(\mathbf{u}^f; \mathbf{u}^i; T) P_{\text{st}}(\mathbf{u}^i); \quad (1.14)$$

The action is a central concept in the weak noise canonical phase space approach and provides a dynamical weight function and selection criteria for a dynamical nonequilibrium process in a similar manner as the energy E in the Boltzmann-Gibbs factor $P \propto \exp[-E]$, (β is the inverse temperature) for equilibrium processes. The action moreover implies an underlying principle of least action and the Hamiltonian entering S , yielding the field equations (1.6) and (1.7), is given by

$$H = \int d\mathbf{x} p(\mathbf{r}^2 \mathbf{u} + \mathbf{u} \mathbf{r} \mathbf{u} - (\mathbf{r}^2 \mathbf{p})); \quad (1.15)$$

where $H = \int d\mathbf{x} H$.

In addition to the conserved Hamiltonian or energy the translational invariance of H (assuming periodic boundary conditions for \mathbf{u} and for \mathbf{p} , modulus a constant) implies conservation of momentum. Moreover, the conserved noise in Eq. (1.1), corresponding to the term $\mathbf{r}^2 \mathbf{p}$ in Eq. (1.6), yields the local conservation law $\partial_t u + \mathbf{r} \cdot \mathbf{j} = 0$, $\mathbf{j} = \mathbf{r} \mathbf{u} + \mathbf{r} \mathbf{p} - (\mathbf{r}^2 \mathbf{u})$, implying the conservation of the integrated slope field or height offset. The two additional conserved quantities are thus given by

$$Z = \int d\mathbf{x} \mathbf{u} \mathbf{r} \mathbf{p}; \quad (1.16)$$

$$M = \int d\mathbf{x} \mathbf{u}; \quad (1.17)$$

We note that the integrated noise field \tilde{P} is not conserved for $\epsilon \neq 0$. According to Eq. (1.6) \tilde{P} evolves according to, see also [4],

$$\frac{d\tilde{P}}{dt} = \int d\mathbf{x} \mathbf{u} \mathbf{r} \mathbf{p}; \quad (1.18)$$

$$\tilde{P} = \int d\mathbf{x} \mathbf{p}; \quad (1.19)$$

The long time-large distance scaling properties of a growing interface is a fundamental issue which has been addressed extensively [17, 18, 24, 25, 26, 27, 28, 29, 30, 31, 32, 33, 34]. For the width $w(L; t)$ of an interface of size L the dynamical scaling hypothesis [22, 35] asserts that $w = L^{-\zeta} G(t=L^\zeta)$ which for the stationary slope correlations corresponds to the

asymptotic scaling form

$$h(u; t) = x^{2-\alpha} F\left(\frac{t}{x^z}\right); \quad (1.20)$$

with roughness exponent $\alpha = 1/2$, dynamical exponent z , and universal scaling function $F(w)$. In one dimension the scaling exponents for the noisy Burgers equation are known exactly [18, 22]. The roughness exponent $\alpha = 1/2$ follows from the known stationary distribution, an effective fluctuation-dissipation theorem, [36]

$$P_{st}(u) \sim \exp\left(-\int^u dx u^2\right); \quad (1.21)$$

whereas the dynamical exponent $z = 3/2$ is a consequence of the scaling law

$$\alpha + z = 2; \quad (1.22)$$

implied by Galilean invariance [17, 18]. It was an important result of the analysis in papers II and III, see also [4], that the dynamical exponent $z = 3/2$ also enters in the dispersion law $E \sim k^{-z}$ for the noise-induced left hand soliton and thus is a feature of the gapless nonlinear excitations providing the many body description of a growing interface.

The description of the stochastic nonequilibrium dynamics of a growing interface can be accessed on two levels: The Langevin level defined by Eqs. (1.1) and (1.5) or the Fokker-Planck level (or Master equation level for discrete models) characterized by the Fokker-Planck equation associated with the Burgers equation,

$$\frac{\partial P}{\partial t} = -H P; \quad (1.23)$$

Here the Hamiltonian or Liouvillian H is given by Eq. (1.15), with the momentum variable p interpreted as the functional derivative $p = \delta/\delta u$, see also [4].

On the Langevin level the growth problem is defined by a stochastic nonlinear differential equation. Apart from direct numerical simulations the standard analytical tool as regards scaling properties is a perturbative renormalization group scheme based on an expansion in powers of the nonlinear term in Eq. (1.1) or Eq. (1.4) [11, 17, 18]. This procedure yields renormalization group equations in an ϵ -expansion about $d = 2$, $\epsilon = d - 2$, predicts a kinetic phase transition above $d = 2$ from a smooth Edwards-Wilkinson phase ($\alpha = (2 - d)/2; z = 2$) to a rough Burgers-KPZ phase with nontrivial exponents. In $d = 1$ the scheme yields (fortuitously) the exact exponents $\alpha = 1/2$ and $z = 3/2$. The limitation of the Langevin

description is that it does not provide a simple physical picture of a growing interface and that the role of the noise can only be discussed and interpreted on a qualitative level.

On the Fokker-Planck level the growing interface is determined by the deterministic evolution equation (1.23) driven by the Hamiltonian (1.15). The formal structure of Eq. (1.23) is equivalent to a functional Schrödinger equation in Wick-rotated imaginary time and allows via the Martin-Siggia-Rose functional integral for a mapping of the growth problem onto a non-Hermitian quantum field theory as discussed in paper II, see also [4]. The quantum field formulation, in addition to also providing an alternative framework for perturbative dynamical renormalization group theory following for example the Callen-Symanzik scheme [37], permits two new lines of approach to the growth problem. Firstly, by a mapping of the Martin-Siggia-Rose path integral onto a directed polymer in a quenched random medium [18, 22] the nonequilibrium problem becomes equivalent to a disorder problem affording a different perspective on the growth problem and yielding new insight. The second line of approach which we adhere to in the present context is to discuss the non equilibrium problem directly in terms of field theoretical constructs. The original stochastic fluctuations on the Langevin level are then interpreted as quantum fluctuations on the Fokker-Planck level, where the noise strength in Eqs. (1.23) serves the role of an effective Planck constant.

In the context of canonical quantization the quantum field theory or quantum many body theory for the interface is defined by Eq. (1.15) with the canonical momentum $p = \partial \phi / \partial \dot{x} = u$ replaced by the momentum operator $\hat{p} = -i \partial / \partial x = u$ in a u -diagonal basis obeying the canonical commutation relation $[\hat{\phi}(x); \hat{u}(x)] = i \delta(x - x')$. In the Edwards-Wilkinson case for $\epsilon = 0$ we are dealing with a free field theory and the elementary excitations or (undressed) quasi-particles are the linear non-propagating dispersive modes with quadratic dispersion $\omega = k^2$, yielding according to spectral properties the dynamic exponent $z = 2$, defining the Edwards-Wilkinson universality class. As discussed in paper II it is also an easy task to evaluate e.g., the slope correlations (1.14) as a purely quantum many body calculation. In the nonlinear Burgers case for $\epsilon \neq 0$ we obtain correction to the linear mode dispersion law. Moreover, the quasi-classical analysis for $\epsilon \neq 0$ in papers II and III also identifies a nonlinear soliton excitation with dispersion law $\omega = k^2 / (1 + \epsilon k^2)$. A detailed analysis of the non-Hermitian quantum field theory has, however, not yet been achieved and will be considered elsewhere.

In the present paper we continue our investigation of the noisy Burgers equation for the

nonequilibrium growth of an interface. We make use of the weak noise canonical phase space approach developed in paper III and consider the following important issues: i) The detailed growth morphology based on the multi-soliton many body description, ii) the non-Hermitian properties of the superimposed linear mode spectrum and the phenomenon of dynamical pinning and mode transmutation, and iii) the correlations in the Edwards-Wilkinson case, the anomalous diffusion of growth modes and switching and pathways in the Burgers-KPZ case, correlations in the multi-soliton sector, and correlations and scaling in the two-soliton sector. With respect to i) we stress that one of the advantages of the quasi-classical weak noise phase space approach propounded in papers II and III is that it provides a many body description of a growing interface in terms of solitons and linear modes. The Landau quasi-particle picture emerging on the Fokker-Planck level was discussed heuristically in paper II. Here we analyze in more detail the time evolution of a growing interface in terms of its elementary excitations. Regarding ii) we note that superimposed on the nonlinear solitons are linear modes obtained by a linear stability analysis of Eqs. (1.6) and (1.7) about a soliton mode. An analysis of the linear mode spectrum was initiated in paper I and II. In the present paper we complete the analysis also for a multi-soliton state and demonstrate among other properties that the linear modes subject to the nonlinear soliton modes undergo a mode transmutation from diffusive non-propagating behavior in the absence of solitons to propagating behavior in the soliton case. Finally, with regard to iii) on the scaling properties of the slope correlations (1.14) we provided in paper II only a heuristic expression for the scaling function \tilde{F} based on a general spectral representation. Here we amend this situation and present an explicit expression for \tilde{F} within the two-soliton approximation. For brief accounts of the present work we refer to [34, 38]; moreover, the papers [39] and [40] present a numerical analysis of the soliton-bearing mean field equations and a tutorial review, respectively.

The paper is organized in the following manner. In Sec. II we discuss the growing interface in terms of soliton modes, in Sec. III we consider the superimposed linear mode spectrum and discuss the mode transmutation alluded to above, in Sec. IV we address the statistical properties, and consider the anomalous diffusion of growth modes, switching and pathways, correlations in the multi-soliton sector, and in detail the correlations in the tractable two-soliton sector. In Sec. V we present a summary and a conclusion.

II. A G R O W I N G I N T E R F A C E

A growing interface governed by the noisy Burgers equation (1.1) is a simple prototype of an intrinsically open and driven nonequilibrium system. In the noiseless case for $\epsilon = 0$ the interface is damped and the slope field u evolves subject to a transient pattern formation consisting of propagating and merging right hand solitons connected by ramp solutions, with superimposed damped linear modes [1, 41]. The motion is deterministic and non-fluctuational. At long times the solitons die out on a time scale set by $1 = k^2$, where k is the dispersive mode wavenumber. In the noisy case for $\epsilon \neq 0$ the time evolution and pattern formation change. The noise balances the damping and drives after a transient period the slope field into a stationary morphology composed of amplitude-matched right and left hand solitons with superimposed linear modes. The noise strength ϵ is an essential parameter changing the qualitative morphology of an interface; this is reflected mathematically in Eq. (1.11) for the transition probability which has an essential singularity for $\epsilon \rightarrow 0$.

The above behavior is illustrated in the linear case where an explicit solution of Eq. (1.1) for a wavenumber component u_k , $u_k(t) = \int_{-\infty}^{\infty} dx u(x;t) \exp(-ikx)$, of the slope field driven by the noise wavenumber component η_k is given by

$$u_k(t) = u_k^i e^{-!_k t} \int_0^t dt' \text{like } !_k(t-t') u_k(t') : \quad (2.1)$$

Here $!_k = k^2$ is the dispersive mode dispersion law and $u_k^i = u_k(t=0)$ the initial slope value. We notice that generally $1 = !_k$ sets the time scale. Initially the motion is deterministic and governed by the noiseless diffusion equation; at longer times for $!_k t \gg 1$ the noise gradually picks up the motion as indicated by the kernel $\exp[-!_k(t-t')]$ in Eq. (2.1) and u_k begins to fluctuate and is driven into a stationary noisy state. This behavior is in accordance with the phase space behavior discussed in paper III on the Fokker-Planck level. In Fig. 1 we have for a particular noise realization depicted the behavior of u_k . We emphasize that the general aspects of the noise-induced time evolution also holds in the noisy Burgers case here subject to a soliton-induced pattern formation. The transient regime is indicated by I, the long time stationary regime by II.

As mentioned above the quantum mechanical interpretation allows a discussion of the growing interface in terms of a Landau quasi-particle picture. In the Edwards-Wilkinson or noninteracting case the relevant quasi-particle is the dispersive mode u_k with quadratic

dispersion law $\omega = k^2$. In the Burgers case it is a general feature of the Landau quasi-particle picture that interactions usually give rise to a dressing effect of the free (bare) quasi-particle, e. g., the inducement of an effective mass. In the diffusive mode case this corresponds to a dressing of the damping constant leaving the dynamical exponent $z = 2$ in $\omega = k^2$ unaltered. However, as shown in papers II and III even for weak α a new quasi-particle emerges, the nonlinear soliton excitation, with dispersion law $\omega / \nu = (\nu^{-1/2})k^{3/2}$.

From a heuristic point of view we can regard the soliton as a self-bound state of diffusive modes; in other words, the solitons condense or nucleate out of the diffusive mode field. We note, however, that while the formation of localized soliton modes with superimposed linear modes is a well-known feature of deterministic evolution equations, e.g., the sine-Gordon equation and the nonlinear Schrödinger equation [42], the underlying mechanism of the doubling of soliton modes here is the noise. In the approach in [4] the soliton mode was identified as a special solution of the classical field equations (1.6) and (1.7) obtained in the limit $\hbar \rightarrow 0$ from i) in [4] the underlying Heisenberg field equations pertaining to the quantum description and ii) in papers II and III from the classical field equations arising from a principle of least action in the WKB limit of the Fokker-Planck description. Below we turn to a discussion of the fluctuating interface in terms of the quantum/classical picture discussed above.

A. The Edwards-Wilkinson case – equilibrium interface

In the Edwards-Wilkinson case [23, 35] the slope of a fluctuating interface is governed by the driven conserved diffusion equation

$$\frac{\partial u}{\partial t} = -\nu \nabla^2 u + \eta; \quad (2.2)$$

which is readily solved both on the Langevin level in Eq. (2.1) and on the Fokker-Planck level. Since the damping term $-\nu \nabla^2 u$ in Eq.(2.2) can be derived from a thermodynamic free energy $F = (\nu/2) \int dx \nabla u^2$ the driven diffusive equation describes an interface in equilibrium at a temperature $T = \nu/2$. In accordance with the quantum field interpretation outlined above, this simple case, however, serves as an illustration of the quasi-particle representation. Consequently, we turn to the field equations (1.6) and (1.7) in the linear case for $\alpha = 0$:

$$\frac{\partial u}{\partial t} = -\nu \nabla^2 u - \nabla^2 p; \quad (2.3)$$

$$\frac{\partial p}{\partial t} = -r^2 p; \quad (2.4)$$

For a single wavenumber component Eq. (2.2) corresponds to a noise-driven overdamped oscillator with force constant $\gamma_k = -k^2$ and the associated canonical field equations (2.3) and (2.4) were solved and discussed in paper III. We find, supplementing the analysis in paper III, the solutions

$$u_k(t) = \frac{u_k^f \sinh \gamma_k t + u_k^i \sinh \gamma_k (T-t)}{\sinh \gamma_k T}; \quad (2.5)$$

$$p_k(t) = e^{-\gamma_k t} \frac{u_k^f u_k^i e^{\gamma_k T}}{\sinh \gamma_k T}; \quad (2.6)$$

for an orbit from u_k^i to u_k^f in time T , $0 < t < T$. The noise field $p_k(t)$ is slaved to the motion of u_k and determined by u_k^i , u_k^f , and T . During the time evolution it evolves from $p_k^i = [u_k^f - u_k^i \exp(-\gamma_k T)] / \sinh \gamma_k T$ to $p_k^f = [u_k^f \exp(\gamma_k T) - u_k^i] / \sinh \gamma_k T$.

We note the correspondence between the physical interpretation on the Langevin level given by Eq. (2.1) and on the Fokker-Planck level characterized by Eqs. (2.5) and (2.6). In the noiseless case for $\gamma = 0$, corresponding to setting $p_k = 0$, i.e., $u_k^f = u_k^i \exp(-\gamma_k T)$, the slope field is damped according to $u_k(t) = u_k^i \exp(-\gamma_k t)$ over a time scale $1/\gamma_k$. In the presence of noise the growing noise field $p_k / \exp(\gamma_k t)$ eventually drives u_k , i.e., $u_k / \exp(\gamma_k t)$. Generally, u_k is a linear combination of a damped part $\exp(-\gamma_k t)$ and a growing part $\exp(\gamma_k t)$, analogous to the decomposition of the field in positive and negative frequency parts in quantum many body theory [43]. Here the components are decaying and growing according to the transient and stationary regimes I and II in Fig. 1, respectively.

The orbit $(u_k; p_k)$ given by Eqs. (2.5) and (2.6), representing the quasi-particles in the classical limit $\hbar \rightarrow 0$, is confined to a submanifold in phase space delimited by four global conservation laws: Conservation of energy $E = H$, conservation of momentum P , conservation of area, i.e., the integrated slope M or height of set; and here also conservation of the integrated noise field P' given by Eqs. (1.15), (1.16), (1.17), and (1.18) for $\gamma = 0$, respectively. In wavenumber space we have

$$E = \int \frac{dk}{2} E_k = \int \frac{dk}{4} k^2 p_k (p_k - 2 u_k); \quad (2.7)$$

and the energy decomposes in contributions E_k for each wavenumber mode k . Inserting Eqs. (2.5) and (2.6) we obtain specially

$$E_k = \frac{\gamma_k^2 [u_k^f]^2 + [u_k^i]^2 - 2 u_k^f u_k^i \cosh \gamma_k T}{2 \sinh^2 \gamma_k T}; \quad (2.8)$$

and the energy only depends on the initial and final configurations u_k^i, u_k^f and the time interval T . For fixed u_k^i and u_k^f and in the long time limit $T \rightarrow \infty$ the energy $E_k \rightarrow 0$ and the orbit migrates to the zero energy manifolds: $p_k = 0$, the transient noiseless submanifold, and $p_k = \pm 2 u_k$, the stationary noisy submanifold. The orbit thus asymptotically passes through the saddle point $(u_k, p_k) = (0, 0)$ where the diverging waiting time ensures ergodic behavior. In Fig. 2 we have depicted the orbits in (u_k, p_k) phase space.

In a similar manner, the momentum decomposes according to

$$p_k = \int_{-u_k}^{u_k} \frac{dk}{2} = \int_{-u_k}^{u_k} \frac{dk}{2} i k u_k p_k : \quad (2.9)$$

We note that p_k vanishes on the zero-energy manifolds $p_k = 0$ and $p_k = \pm 2 u_k$; in the latter case since the integral in Eq. (2.9) becomes a total derivative. For a finite time orbit insertion of Eqs. (2.5) and (2.6) explicitly yields

$$p_k = \frac{\text{Im}(u_k^i u_k^f)}{\sinh \frac{1}{2} k T}; \quad (2.10)$$

in terms of u_k^i, u_k^f , and T ; for $T \rightarrow \infty$ we have $p_k \rightarrow 0$. Likewise for the integrated slope and noise field, $P = \pm 2 M$, we have

$$M = \int_{-u_k}^{u_k} dx u^i(x) = u_{k=0}^i; \quad (2.11)$$

Finally, the action associated with an orbit is obtained from Eq. (1.10). Inserting the equation of motion Eq. (2.3) we have as an intermediate result $S = (1/2) \int_{-u_k}^{u_k} dk S_k$, $S_k = (1/2) \int_{-u_k}^{u_k} dt k^2 \dot{p}_k^2$ and using Eq. (2.6) the action

$$S = \int_{-u_k}^{u_k} \frac{dk}{2} \frac{j u_k^f - u_k^i \exp(-\frac{1}{2} k T)}{\exp(-\frac{1}{2} k T)}; \quad (2.12)$$

determined by the initial and final configurations u_k^i and u_k^f and the traversal time T . According to Eq. (1.11) we subsequently obtain the transition probability

$$P(u_k^f; u_k^i; T) / \exp \left[- \int_{-u_k}^{u_k} \frac{dk}{2} \frac{j u_k^f - u_k^i \exp(-\frac{1}{2} k T)}{\exp(-\frac{1}{2} k T)} \right]; \quad (2.13)$$

a well-known result [44, 45]). In the limit $T \rightarrow \infty$ the orbit migrates to transient-stationary zero-energy manifolds and we arrive at the stationary Gaussian distribution (1.21). This behavior in phase space is consistent with the qualitative behavior shown in Fig. 1.

Summarizing, in the linear Edwards-Wilkinson case the conserved noise-driven stochastic diffusion equation is in the weak noise limit equivalent to coupled field equations admitting

both damped and growing solutions for the slope field. The stochastic noise is replaced by a noise field canonically conjugate to the slope field. Both damped and growing solutions are required in order to describe the crossover from the transient regime to the stationary regime. The wavenumber k is a good quantum number and we can envisage the fluctuating interface as a gas of growing and damped dispersive modes according to the decomposition, see also paper II,

$$u(x;t) = \int \frac{dk}{2} [A_k e^{-ikx} e^{-\Gamma_k t} + B_k e^{ikx} e^{\Gamma_k t}] \quad (2.14)$$

In field theoretical terms $u(x;t)$ is a free field and the elementary modes are noninteracting. A particular mode lies on the energy surface E_k and is moreover specified by the conserved momentum p_k . Furthermore, under time evolution the integrated slope field M and noise field P are also conserved. Finally, with the mode is associated an action S_k yielding the transition probability P .

The description based on the field equations (2.3) and (2.4) and the associated symplectic structure is basically classical. Subject to canonical quantization the dispersive modes become bona fide elementary excitations and a Landau quasi-particle picture of the interface emerges. The original noise fluctuations are then interpreted as quantum fluctuations emerging from the underlying operator algebra. Finally, we note that subject to a Wick rotation $t \rightarrow i\tau$ the dispersive quasi-particles are transformed to dispersive particle-like quasi-particles with mass $m = 2$.

B. The Burgers-KPZ case - nonequilibrium interface

In the case of a growing interface the situation is more complex. The general behavior depicted in Fig. 1 still holds in the sense that the interface evolves from a transient state to a stochastic stationary state. However, unlike the linear equilibrium case where the fluctuations in u are extended and dispersive, the fluctuations in the nonlinear nonequilibrium growth case include localized propagating modes in order to account for a growing height profile. This is also evident from e.g., the KPZ equation in Eq. (1.4), where the damping and growth terms transform differently under time reversal. For $t \rightarrow -t$, $h \rightarrow h + \lambda t$, and $\lambda \rightarrow -\lambda$ the KPZ equation stays invariant. This is consistent with the fact that in the decomposition of the irreversible linear modes in growing and decaying components the

damping enters in the combination ∂_t , whereas the average nonlinear reversible growth term in the stationary state $\partial_t h = \partial_t i_{st} = (-2)h(xh)^2i$ is invariant. Clearly, the growth term cannot be derived from a thermodynamic free energy, the term moreover violates the potential condition [46, 47, 48, 49] and drives the system away from thermal equilibrium into a stationary kinetic growing state.

The issue on the Fokker-Planck level is again to establish a quasi-particle picture and to determine orbits in $(u;p)$ phase space from an initial configuration u^i at time $t=0$ to a final configuration u^f at time $t=T$ in order to, via the action associated with the orbit, evaluate the transition probability $P(u^f;u^i;T)$. The orbit is in principle determined as an initial-final value problem, i.e., a boundary value problem in time, of the mean field equations (1.6) and (1.7). Unlike the linear case where we can expand u on plane wave dispersive modes and thus achieve a complete analysis, the nonlinear and presumably nonintegrable character of Eqs. (1.6) and (1.7) precludes such an analysis.

Two new features distinguish the field equations (1.6) and (1.7) from the linear case: i) the nonlinear coupling strength setting together with an intrinsic length scale λ and ii) the amplitude-dependent Galilean invariance (1.3). The new length scale allows for the possibility of localized nonlinear excitations and the Galilean symmetry permits the generation of a class of propagating particle-like excitations from a static solution, i.e., an excitation at rest. The static excitations are the right and left hand solitons (1.8) characterized by the parity index $\sigma = \pm 1$. Boosting a static soliton to the velocity v , denoting the boundary values u_+ and u_- , and using the Galilean symmetry in (1.3) we obtain the fundamental soliton condition

$$u_+ + u_- = \frac{2v}{\lambda} \quad (2.15)$$

In Fig. 3 we have depicted the fundamental "quarks" or solitons and the associated height profiles.

The right hand soliton for $\sigma = +1$ moves on the noiseless transient submanifold $p = 0$ and is a solution of the damped noiseless Burgers equation, i.e., Eq. (1.1) for $\eta = 0$. Within the canonical framework the right hand soliton does not contribute to the dynamics of the interface; according to Eqs. (1.15) and (1.16) with $p = 0$ it carries zero energy and zero momentum. The left hand soliton for $\sigma = -1$ is associated with the noisy or stationary submanifold $p = 2u$ and it follows from the field equations that it is a solution of the

growing noiseless Burgers equation for $\nu = 0$. Note that due to the uneven boundary values u_+ and u_- the solitons are self-sustained dissipative structures driven by boundary currents as discussed in paper I. The left hand soliton is endowed with dynamical attributes and carries according to Eqs. (1.15), (1.16), and (1.10) energy, momentum, and action:

$$E = \frac{2}{3} (u_+^3 - u_-^3); \quad (2.16)$$

$$= (u_+^2 - u_-^2); \quad (2.17)$$

$$S = \frac{1}{6} (ju_+ - u_-^2)T; \quad (2.18)$$

Since $u_+ < u_-$ for a left hand soliton its energy is negative. Expressing u in the form $u = (2\nu = \epsilon)(u_+ - u_-)$ using Eq. (2.15) it follows that ϵ points in the direction of v . From $\epsilon = mv$ we can also associate an amplitude-dependent mass $m = (2 = \epsilon)ju_+ - u_-^2$ with the soliton. Finally, the action for a left hand soliton orbit over time T is positive and Galilean invariant.

In addition to the localized soliton modes the field equations also support linear modes superimposed on the soliton. These modes are obtained by a linear stability analysis of the field equations and will be discussed in Sec. III. In the limit $\nu \rightarrow 0$ the soliton modes vanish and the remaining fluctuations are the dispersive modes of the Edwards-Wilkinson model.

The field equations (1.6) and (1.7) are nonlinear and the soliton solutions do not constitute a complete set in the same manner as the plane wave decomposition (2.14) in the Edwards-Wilkinson case. We shall nevertheless as a working hypothesis assume that we can resolve a given initial interface slope profile u in terms of a gas of right hand and left hand solitons matched according to the soliton condition (2.15); i.e., with horizontal constant slope segments. Associated with the soliton representation of u there is also a soliton representation of the associated noise field p . From the form of the field equations it follows that a multi-soliton configuration is an approximate solution provided we can control the overlap contribution $u^i r u^l$ arising from the nonlinear term; here i and l denote the i -th and l -th soliton. Since the soliton width is of order $\epsilon = u$ the overlap only contributes in a region of order $\epsilon = u$ about the soliton center and is small in the inviscid limit $\nu \rightarrow 0$ and for a dilute soliton gas. Otherwise, we assume that at least for small ν we can absorb the correction term in a linear mode contribution. In summary, we represent a slope configuration u and the associated noise field configuration p in terms of a gas of right hand and left hand solitons matched according to Eq. (2.15) with superimposed linear modes.

This representation of a growing interface is in the spirit of a Landau quasi-particle picture of an interacting quantum many body system [43, 50]. In a heuristic sense we assume that the interface at a given instant of time is characterized by a gas of localized soliton modes and extended linear modes. Since the soliton is not associated with a particle but is a nonlinear solution of classical field equations the soliton number is not conserved; in other words, solitons are created and annihilated subject to collisions.

Keeping only the solitons, explicit expressions for u and p are easily constructed in terms of the Galilee-boosted soliton modes (1.8). Introducing the mean amplitude k_p and velocity v_p in terms of the boundary value u_{p+1} and u_p of the p -th soliton,

$$k_p = \frac{1}{4} (u_{p+1} - u_p); \quad (2.19)$$

$$v_p = \frac{1}{2} (u_{p+1} + u_p); \quad (2.20)$$

we obtain for an n -soliton representation of the slope field u_s and associated noise field p_s

$$u_s(x;t) = \sum_{p=1}^{X^n} k_p \tanh j_p j(x - v_p t - x_p); \quad (2.21)$$

$$p_s(x;t) = \sum_{p=1, k_p < 0}^{(2)^2 X^n} k_p \tanh j_p j(x - v_p t - x_p); \quad (2.22)$$

The solitons are arranged from left to right according to the increasing index $p, p = 1; 2; \dots, n$.

The center of the p -th soliton is at x_p and we have set $u_1 = u_{n+1} = 0$. In Fig. 4 we have shown an n -soliton configuration.

The soliton representation in Eq. (2.21) of the interface evolves in time according to the field equations. The motion corresponds to an orbit in $(u;p)$ phase space lying on the manifold determined by the conservation of energy E , momentum P , and area M according to Eqs. (1.15), (1.16), and (1.17). We also observe from Eq. (1.18) that the integrated noise field P^* , since \mathcal{H} is conserved, develops linearly in time according to

$$P^* = \mathcal{H} t + \text{const}; \quad (2.23)$$

In the soliton representation the contributions to the energy, momentum, action, and area decompose. Noting that only left hand solitons for $u_{p+1} < u_p$ contribute dynamically we have applying Eqs. (2.16), (2.17), (2.18) and (1.17)

$$E = \sum_{p=1, u_{p+1} < u_p}^{X^n} \frac{2}{3} (u_{p+1}^3 - u_p^3); \quad (2.24)$$

$$= \sum_{p=1}^N \int_{u_{p+1} < u_p} (u_{p+1}^2 - u_p^2); \quad (2.25)$$

$$S = \frac{1}{6} T \sum_{p=1}^N \int_{u_{p+1} < u_p} (u_{p+1}^3 - u_p^3); \quad (2.26)$$

$$M = \sum_{p=1}^N u_{p+1} (x_{p+1} - x_p); \quad (2.27)$$

Although, as follows from Eqs. (2.24), (2.25), and (2.26), the total energy, momentum, and action are additive quantities (extensive) the soliton gas still represents a very intricate many body problem. This is due to the soliton matching condition in Eq. (2.15), i.e., the horizontal segments connecting the solitons, and the dynamical asymmetry between left hand and right hand solitons. The solitons in the representation (2.21) propagate with in general different velocities v_p and are thus subject to collisions. Since we only have at our disposal single soliton solutions of the field equations patched together to represent a slope configuration at a particular time instant and not a general solution we have limited control over soliton-soliton scattering. Clearly, the expressions (2.24 - 2.26) only hold in-between soliton collisions. In particular, the time T entering in the action (2.26) refers to times between collisions, i.e., T is typically of order $|x_{p+1} - x_p|/v_p$. The working assumption here is that in-between collisions the soliton (plus linear modes) representation is valid and that energy, momentum, and area are conserved during collisions. However, the number of solitons is not preserved, i.e., solitons are created and annihilated subject to collisions. Finally, we note that at long times the orbit from u^i to u^f migrates to the zero-energy manifold as conjectured in paper III. This implies that the finite energy solitons at long times are suppressed and that the system in this limit is described by dispersive modes yielding the stationary distribution (1.21). For further illustration we have in Fig. 5 depicted the slope field u , height field h , and noise field p for a 4-soliton configuration. The solitons are centered at x_1, x_2, x_3 , and x_4 and propagate with velocities $v_1 = (-2)u_2$, $v_2 = (-2)(u_3 + u_2)$, $v_3 = (-2)(u_4 + u_3)$, and $v_4 = (-2)u_2$, where u_2, u_3 , and u_4 are the plateau values. The configuration carries energy $E = (2/3)(u_2^3 - u_3^3)$, momentum $P = (u_2^2 - u_3^2)$, action $S = (1/6) T (u_2^3 + u_4^3 - u_3^3 + u_4^3)$, and area $M = u_2(x_2 - x_1) + u_3(x_3 - x_2) + u_4(x_4 - x_3)$ at time $t = 0$. By integration we note that the total noise field P evolves like $P = P_0 + t(u_2^2 - u_3^2)$ in agreement with Eq. (2.23).

It is clear that the nonequilibrium growth of the interface is fundamentally related to the

existence of localized propagating soliton modes. Expressing the KPZ equation (1.4) in the form

$$\frac{\partial h}{\partial t} = -r^2 h + \frac{1}{2} u^2 + \dots; \quad (2.28)$$

the linear damping term is associated with the linear modes, whereas the nonequilibrium growth term is driven by the solitons. In the Edwards-Wilkinson case the modes are extended and dispersive, $u \propto \sum_k f_k(t) \cos(kx + \phi)$, where $f_k(t)$ is related to Eq. (2.5), and the height field $h = \int^x u dx^0$ for a particular k -mode behaves like $h \propto \sin(kx + \phi)$; consequently, $\langle \dot{h} \rangle = 0$ and growth is absent. On the contrary, in the Burgers case the localized soliton modes emerge and $h(x) = \int^x u(x^0) dx^0$ grows owing to the propagation of solitons across the system. Averaging Eq. (2.28) and setting $\partial_t = 0$ we have $\langle \dot{h} \rangle = -\langle r^2 \rangle h + \text{const.}$ which is consistent with the passage of a soliton with amplitude u and velocity $|v| = \langle r^2 \rangle u$ at a given point x . This growth behavior also follows from inspection of Fig. 5.

The constant slope and noise field configuration $u = u_0$ and $p = p_0$ have according to Eqs. (1.15) and (1.16) vanishing energy E and momentum and thus form a continuum of zero-energy states; note that the energy is not bounded from below, i.e., the zero-energy states are not ground states. The right and left hand solitons in Eq. (1.8) lift the zero-energy degeneracy and connect a constant u_- configuration to a constant u_+ configuration. Unlike the solitons in the ϕ^4 theory or sine-Gordon theory [42, 51], connecting two degenerate ground states ϕ_0 or degenerate ground states $\phi_0 = p$, where p is an integer, respectively, with massive gapful excitations, the Burgers solitons are gapless modes forming a continuum of states with energy $E \propto (u_+^3 - u_-^3)$ and momentum $\propto (u_+^2 - u_-^2)$.

In the discussion of a growing interface in terms of its slope field we must introduce appropriate boundary conditions in order to describe the physical growth state. In the instantaneous configuration in Figs. 4 and 5 we chose for convenience vanishing slope at the boundaries. However, owing to the soliton propagation this boundary condition cannot be maintained in the course of time as the solitons cross the boundaries of the system and it is more appropriate to assume periodic boundary conditions for the slope field, i.e., $u(x) = u(x + L)$ at all times, where L is the size of the system. Note that periodic boundary conditions for the slope field in general does not imply periodic boundary conditions for the associated height field h , the integrated slope field. We have from $h(x) = \int^x u(x^0) dx^0$, $h(x) = h(x + L) + M$, where M is the area under u , and only in the case of zero-area slope

configurations does h also satisfy periodic boundary conditions, corresponding to vanishing height offset at the boundaries.

Whereas periodic boundary conditions for the slope field are consistent with the extended dispersive modes in the Edwards-Wilkinson case, i.e., the free fields, the elementary right and left hand Burgers solitons violate the boundary conditions since they connect unequal zero-energy states. In this sense we can regard the solitons as "quarks" in the present many body formulation. A proper elementary excitation or quasi-particle satisfying periodic boundary conditions is thus composed of two or more "quarks" as illustrated in Figs. 4 and 5.

1. The two-soliton configuration

The simplest configuration satisfying periodic boundary condition is composed of two solitons of opposite parity, i.e., a noisy and a noiseless kink. The solitons have the common amplitude u , are centered at x_1 and x_2 and propagate as a composite entity, according to Eq. (2.15) with velocity $v = \pm u/2$. Specifically, this pair-soliton mode has the form

$$u_2(x;t) = \frac{u}{2} \tanh \frac{k_s}{2} (x - vt - x_1) - \tanh \frac{k_s}{2} (x - vt - x_2) : \quad (2.29)$$

The configuration u_2 together with the associated noise field p_2 (for $u > 0$)

$$p_2(x;t) = \frac{u}{2} \left[1 - \tanh \frac{k_s}{2} (x - vt - x_1) \right] ; \quad (2.30)$$

and the height field h_2

$$h_2(x;t) = \frac{u}{k_s} \log \frac{\cosh \frac{k_s}{2} (x - vt - x_1)}{\cosh \frac{k_s}{2} (x - vt - x_2)} + \text{const.} \quad (2.31)$$

are depicted at the initial time $t = 0$ in Fig. 6

According to Eqs. (2.24 - 2.27) the two-soliton configuration is endowed with the dynamical attributes:

$$E = \frac{2}{3} u^3 ; \quad (2.32)$$

$$= \text{sign}(u) u^2 ; \quad (2.33)$$

$$S = \frac{1}{6} u^3 T ; \quad (2.34)$$

$$M = u(x_2 - x_1) ; \quad (2.35)$$

The two-soliton configuration corresponds to an orbit in $(u;p)$ phase space. Choosing as initial configuration at $t = 0$ $(u^i; p^i) = (u_2(x;0); p_2(x;0))$ the final configuration at $t = T$ is then given by $(u^f; p^f) = (u_2(x;T); p_2(x;T))$. In a finite system of size L with periodic boundary conditions this is moreover a periodic orbit with period $L=v$; in the thermodynamic limit $L \rightarrow \infty$ the period diverges.

By inspection of Fig. 6 it follows that the two-soliton configuration propagates with a constant profile preserving the area M , i.e., the height of set $2u(x_2 - x_1)$. Subject to periodic boundary conditions in a system of size L the soliton pair reappears after a period $L=v$. This motion corresponds to a simple growth scenario where a layer of thickness $h = u(x_2 - x_1)$ is added to h per revolution of the pair. Subject to this particular soliton mode the interface thus grows with velocity $(1/2) u^2(x_2 - x_1) = L$. This is consistent with the averaged form of Eq. (2.28) in the stationary state, $h @ h @ t = (1/2) h u^2$, noting the spatial weight $(x_2 - x_1) = L$ of the soliton pair in the average $h @ h @ t$ over the interface. We also remark that the local increase in h , $\dot{h} = u \dot{\ell}$, owing to the passage of a soliton pair of size $\ell = |x_2 - x_1|$ in time $t = \ell/v$, where $v = u/2$, yields $\dot{h} = t = (1/2) u^2$, again in accordance with the averaged KPZ equation. Finally, the integrated noise field $\tilde{P} = \int^R dx p$ decreases linearly with time as the soliton pair revolves like $\tilde{P} = \tilde{P}_0 - 4 u |\dot{u}| t$ in agreement with Eq. (2.23).

According to $v = u/2$ the velocity of the soliton pair is proportional to the amplitude u . Expressing the energy E and momentum in terms of v we have $E = (16/3) (\ell^3) v^3$ and $P = 4 (\ell^2) v^2$ characterizing the nonlinear excitation. Moreover, eliminating the velocity we arrive at the dispersion law

$$E = \frac{4}{3} \frac{1}{1-2} \ell^3 v^{3/2} : \quad (2.36)$$

The soliton pair is thus a gapless quasi-particle mode with exponent $z = 3/2$. As discussed in paper II a general spectral representation for the slope correlations allows us to make contact with the scaling form in Eq. (1.20) and identify the mode exponent z with the dynamic exponent.

Within the present description the statistical weight of the soliton is determined by Eq. (1.21). In the inviscid limit for small ℓ we obtain for a pair of size ℓ and amplitude u the normalized stationary distribution

$$P_{st}(u; \ell) = \frac{1}{Z} (L) \exp \left(-u^2 \ell \right) ; \quad (2.37)$$

with normalization factor

$$P_{st}(L) = 2 \left(\frac{1}{L} \right)^{1/2} L^{1/2} : \quad (2.38)$$

The distribution is parameterized by the amplitude u and the size ℓ . The normalization factor or partition function P_{st} varies as $L^{1/2}$ and the distribution thus vanishes in the thermodynamic limit $L \rightarrow \infty$, characteristic of a localized excitation. The mean size of a soliton pair is given by

$$\langle \ell \rangle = \int_0^L \int_0^{\infty} \ell \, d\ell \, du \, P_{st}(u; \ell) : \quad (2.39)$$

Inserting P_{st} we obtain $\langle \ell \rangle = (1/3)L$, i.e., the mean size of the pair scales with the system size. This behavior is characteristic of a spatially extended or loosely bound excitation and we can envisage the soliton pair as a "string excitation" connecting right and left hand solitons (the fundamental "quarks").

In a similar manner we can determine the transition probability associated with a soliton pair using Eq. (1.11). Inserting S from Eq. (2.34) and normalizing we obtain

$$P_{sol}(u; T) = \frac{1}{Z_{sol}(T)} \exp \left(- \frac{1}{6} u^2 T \right) ; \quad (2.40)$$

where the normalization factor or dynamic partition function is given by

$$Z_{sol}(T) = \frac{2}{3} - \frac{1}{3} - \frac{6}{T} \frac{1}{\Gamma} : \quad (2.41)$$

Here the Gamma function $\Gamma(z) = \int_0^{\infty} t^{z-1} \exp(-t) dt$ arises from the normalization of P_{sol} ; $\Gamma(1/3) = 2.68174$.

Before turning to the linear fluctuation spectrum in the next section we wish to briefly review a recent numerical study of the field equations (1.6) and (1.7) [39]. The field equations are of the dispersive-advection type with the characteristic feature that the equation for p admits exponentially growing solutions due to the negative dispersion coefficient thus rendering direct forward integration in time numerically unfeasible. In order to resolve this instability problem we developed a "time loop" integration procedure based on integrating the equation for u forward in time followed by an integration backward in time of the equation for p . This numerical scheme thus requires an assignment of both initial and final (u, p) configurations and therefore mainly served as a tool to check whether a certain assignment actually constitutes a solution.

We investigated numerically three propagating soliton configurations: i) a propagating soliton pair, ii) two symmetrical solitons colliding with a static soliton, and iii) the collision of two symmetrical soliton pairs. Referring to [39] for details we summarize our findings below. We found in case i) that the pair-soliton in the inviscid limit for small ν is a long lived excitation thus justifying the quasi-particle interpretation above. In case ii) we considered symmetrical solitons propagating towards and colliding with a static soliton at the center passing through the static soliton and reemerging with no phase shift or delay; this specific mode corresponds to rolling in a dip and subsequently nucleating a tip at the same point in the height field. In case iii) we finally considered two symmetrical soliton pairs colliding and reappearing subject to a phase shift or delay where the incoming trailing solitons become the leading outgoing solitons; this mode corresponds to rolling in a trough and subsequent nucleation of a plateau in the height profile. It was characteristic of the soliton collisions in case ii) and iii) that the conservation of E , \mathcal{P} , and M was satisfied during collision, a feature that seems to stabilize the integration.

III. FLUCTUATIONS – MODE TRANSFORMATION

The soliton spectrum discussed in the previous section is a fundamental signature of the nonlinear character of the Burgers equation and at the same time essential in accounting for the growth aspects of an interface. In the present section we address the fluctuation spectrum or linear mode spectrum superimposed on the soliton gas. In the linear Edwards-Wilkinson case discussed in Sec. II the fluctuations exhaust the mode spectrum and have a diffusive character. In the nonlinear Burgers-KPZ case the fluctuations are superimposed on the soliton modes and become propagating. The fluctuation spectrum was discussed incompletely in the noiseless Burgers case in paper I and in the noisy case in paper II. Here we present a detailed analysis. A brief account of the work is given in [38]; here we complete the analysis.

A . The noiseless Burgers case

The noiseless Burgers equation is inferred from Eq. (1.1) by setting $\eta = 0$ and also follows from the field equation (1.6) on the $p = 0$ submanifold,

$$\frac{\partial}{\partial t} (ur) + u = r^2 u: \quad (3.1)$$

This equation exhibits a transient pattern formation composed of right hand solitons connected by ramps with superimposed linear modes. A single right hand static soliton mode is given by Eq. (1.8) for $\eta = 1$, i.e., $u_s = u \tanh k_s x$, $k_s = u/2$. The soliton has amplitude u and width k_s^{-1} . A spectrum of moving solitons is then generated by the Galilean boost (1.3): $x \rightarrow x - u_0 t$, $u \rightarrow u - u_0$.

In order to analyze the superimposed linear fluctuations we expand u about the soliton mode u_s , $u = u_s + \delta u$. To linear order in δu we obtain the equation of motion

$$\frac{\partial}{\partial t} (u_s r) + \delta u = r^2 \delta u + (r u_s) \delta u: \quad (3.2)$$

In the asymptotic limit for large $|x|$ this equation is readily analyzed. Noting that $u_s \rightarrow u \text{sign}(x)$, $r u_s \rightarrow 0$, and searching for plane wave solutions of the form $\delta u \propto \exp(-E_k t) \exp(ikx)$ we identify a spectrum of complex eigenvalues,

$$E_k = -k^2 - i u k \text{sign}(x); \quad (3.3)$$

showing the non-Hermitian character of Eq. (3.2). Introducing the phase velocity $v = u$ the imaginary part of the eigenvalue E_k combines with the plane wave part and yields the propagating damped wave form

$$\delta u \propto e^{-k^2 t} e^{ik(x + v t \text{sign}(x))}: \quad (3.4)$$

The soliton mode thus gives rise to a mode transmutation in the sense that the dispersive mode in the Edwards-Wilkinson case $\delta u \propto \exp(-k^2 t) \exp(ikx)$ is transmuted to a damped propagating mode in the Burgers case with a phase velocity v depending on the soliton amplitude u . The mode transmutation, of course, also follows from the Galilean invariance in Eq. (1.3) since a shift of the slope field to the soliton amplitude u corresponds to a transformation to the moving frame $x \rightarrow x - ut$. For large positive x the mode propagates to the left, for large negative x the propagation is to the right, i.e., the mode propagates

towards the soliton center which thus acts like a sink. The phenomenon of mode transmutation has also been noted by Schutz [52] in the case of the asymmetric exclusion model, a lattice version of the noisy Burgers equation, in the context of analyzing the shocks, corresponding to the solitons in the present context.

As noted in paper I the analysis of Eq. (3.2) can be extended to the whole axis by introducing a nonuniform gauge function g determined by the soliton profile in Eq. (1.8),

$$g(x) = k_s \tanh k_s x ; \quad k_s = u/2 : \quad (3.5)$$

By means of g we can express Eq. (3.2) in the Schrodinger-like form

$$\frac{\partial u}{\partial t} = D(g) u ; \quad (3.6)$$

where the operator $D(g)$ in the quantum mechanical analogue is given by the Hamiltonian

$$D(g) = -\frac{1}{2} \left(\frac{\partial}{\partial x} + g(x) \right)^2 + \frac{1}{2} k_s^2 \tanh^2 k_s x : \quad (3.7)$$

This equation of motion describes in imaginary Wick-rotated time a particle moving in the potential $V = \frac{1}{2} \cosh^2 k_s x$ subject to the imaginary gauge field ig . Absorbing the gauge field by means of the gauge transformation

$$U(g) = \exp \int^x g(x) dx = \cosh^{-1} k_s x ; \quad (3.8)$$

and using the identity $(\partial + g)^2 = U(g) \partial^2 U(g)^{-1}$, the non-Hermitian equation of motion (3.6) takes the Hermitian form

$$\frac{\partial \psi}{\partial t} = D(0) \psi ; \quad (3.9)$$

where

$$\psi = U(g)^{-1} u : \quad (3.10)$$

We also observe that the gauge transformation in Eq. (3.8) has the same form as the Cole-Hopf transformation [53, 54] applied to the static soliton solution u_s , see also papers I-III.

The presence of the gauge function changes the spatial behavior of the eigenmodes and thus their normalizability. The imposition of physical constraints such as spatially localized

modes or asymptotic plane wave modes obeying periodic boundary conditions consequently give rise to a complex eigenvalue spectrum. Since we can "gauge" the mode problem in Eq. (3.6) to the exactly solvable Schrodinger problem defined by Eq. (3.9) we are able to complete the analysis.

Setting $\omega = \exp(-t)$, where ω is the frequency eigenvalue, the spectrum of the ensuing eigenvalue problem,

$$D(0)\psi = \omega\psi; \quad (3.11)$$

associated with $D(0)$ can be analyzed analytically [55, 56]. It is composed of a localized zero-frequency mode and a band of phase-shifted extended scattering modes with eigenvalue

$$\omega_k = -(k^2 + k_s^2); \quad (3.12)$$

The eigenmodes have the form

$$\psi_0 = \frac{1}{\cosh k_s x}; \quad \omega_0 = 0; \quad (3.13)$$

$$\psi_k = \exp(ikx)s_k(x); \quad \omega_k = -(k^2 + k_s^2); \quad (3.14)$$

$$s_k(x) = \frac{k + ik_s \tanh k_s x}{k - ik_s}; \quad (3.15)$$

The x -dependent s -matrix $s_k(x) = \psi_k(x)/\psi_0(x)$ gives rise to a spatial modulation $|\psi_k(x)|^2 = [(k^2 + k_s^2 \tanh^2 k_s x)/(k^2 + k_s^2)]^{1/2}$ of the plane wave near the soliton center over a range k_s^{-1} and a phase shift $\theta_k(x) = \tan^{-1}(k_s \tanh k_s x/k) + \tan^{-1}(k_s/k)$. For $x \rightarrow -\infty$, $s_k(x) \rightarrow 1$; for $x \rightarrow \infty$, $s_k(x) \rightarrow (k + ik_s)/(k - ik_s) = \exp(i\theta_k)$, and $s_k(x)$ becomes the usual s -matrix. We note that the bound state solution and its zero-frequency eigenvalue is contained in the scattering solution as a pole in the s -matrix for $k \rightarrow ik_s$.

Inserting the gauge transformation in Eq. (3.8) we obtain for the zero-mode $u = \cosh^{-2}(k_s x)/r u_s$ which thus corresponds to the translation or Goldstone mode associated with the position of the soliton. For the extended states the gauge transformation U provides an envelope of range k_s^{-1} , i.e., $u = \exp(ikx)s_k(x)\cosh^{-1}(k_s x)$. The complete solution of the mode equation (3.2) thus takes the form

$$u = \frac{A}{\cosh^2 k_s x} + \sum_k B_k \exp(ikx) \frac{\exp(ik_s x)}{\cosh k_s x} s_k(x); \quad (3.16)$$

expressing the fluctuations of the slope field about the static right hand soliton u_s ; A and $B_k = B_{-k}$ are expansion coefficients. The first term in Eq. (3.16) is the time independent

translation mode. The second term corresponds to a band of damped localized states with a gap k_s^2 in the spectrum $\omega_k = (k^2 + k_s^2)^{1/2}$. Moreover, the scattering modes are transparent and phase-shifted by $\delta_k = 2 \tan^{-1}(k_s/k)$, implying according to Levinson's theorem that the band is depleted by precisely one state corresponding to the translation mode.

In order to make contact with the asymptotic analysis yielding the spectrum in Eq. (3.3) we observe that the fluctuations given by Eq. (3.16) do not exhaust the spectrum. Since the gauge factor $U = \cosh^{-1} k_s x$ provides a fall-off envelope we can extend the set of solutions by an analytical continuation in the wavenumber k in the same manner as the translation mode is retrieved by setting $k = ik_s$. Thus shifting $k \rightarrow k + i$, where $j \rightarrow k_s$, we obtain by insertion the complex spectrum

$$E_{k,j} = (k^2 + k_s^2 - j^2) + 2i k j; \quad j \geq k_s; \quad (3.17)$$

and associated fluctuation modes

$$u = \frac{A}{\cosh^2 k_s x} + \sum_{k,j} B_{k,j} e^{-(k^2 - j^2)t} e^{ik(x - 2t)} \frac{e^{-x}}{\cosh k_s x} S_{k+j}(x); \quad (3.18)$$

where $B_{k,j} = B_{k,j}^*$ since u is real.

The expressions (3.17) and (3.18) provide the complete analytically continued solution of the fluctuation spectrum about the static soliton compatible with the imposed physical boundary conditions. For $j = k_s$ we recover the spectrum (3.3) of right hand and left hand extended gapless modes propagating towards the soliton center with velocity $v = 2 k_s = u$. For $j < k_s$ we obtain a band of gapful modes with localized envelopes propagating with velocity 2 towards the soliton center. Finally, for $j = 0$ the envelope is symmetric, the spectrum $E_{k,0}$ is real, and the mode has no propagating component; for $k = 0$ and $j = k_s$ we retrieve the time independent translation mode. With the exception of the extended mode for $j = k_s$, the envelope modes for $j < k_s$ are dynamically pinned to the soliton. This phenomenon of localization or dynamical pinning of the modes is associated with the complex spectrum in Eq. (3.17) resulting from the non-Hermitian character of the eigenvalue problem. In all cases the modes are damped with a damping constant given by $(k^2 + k_s^2 - j^2)$. We mention that a non-Hermitian eigenvalue spectrum is also encountered in the context of flux pinning and the transverse Meissner effect in high T_c superconductors [57, 58]. Here the imaginary gauge field is uniform and is given by the applied transverse magnetic field; in the present case the gauge field is spatially varying and given by the nonlinear soliton excitations.

In Fig. 7 we have depicted the spectrum in a plot of the imaginary part of E_k versus its real part. In Fig. 8 we have shown the associated characteristic fluctuation mode patterns. Specifically, in order to obtain a real extended mode propagating towards the soliton center with velocity $v = 2 k_s u$ from the left and with velocity $-v$ from the right with continuous derivative at $x = 0$, thus extending the asymptotic solution (3.4) to the whole axis we form an appropriate linear combination from Eq. (3.18) with equal weights according to the assignments k and $-k_s$. Ignoring here the modulation factor $s_{k+i}(x)$, which is easily incorporated, we obtain

$$u / e^{-k^2 t} = \frac{e^{k_s x} \cos k(x - vt) + e^{-k_s x} \cos k(x + vt)}{\cos k_s x} : \quad (3.19)$$

This mode is depicted in Fig. 9

B. The noisy Burgers case

In order to discuss the fluctuation spectrum in the noisy case we must address the coupled field equations (1.6) and (1.7) and expand the slope field u and noise field p about the soliton configurations, in the single soliton case given by Eqs. (1.8) and (1.9) and in the multi-soliton case by Eqs. (2.21) and (2.22). As also resulting from the analysis in paper II it is convenient to make use of a symmetrical formulation and introduce the auxiliary noise field $'$ by means of the shift

$$p = (u - '): \quad (3.20)$$

The field equations then assume the symmetrical form

$$\frac{\partial}{\partial t} u - u^2 = -r^2 ' ; \quad (3.21)$$

$$\frac{\partial}{\partial t} ' - u^2 = -r^2 u : \quad (3.22)$$

The single soliton solution u_s is given by Eq. (1.8) and the associated noise solution by

$$'_s = u_s + \text{const}: \quad (3.23)$$

Expanding about a general multi-soliton configuration $(u_s; ' _s)$, where u_s is given by Eq. (2.21) and $' _s$ by (modulus a constant)

$$' _s(x;t) = \frac{2}{\pi} \sum_{p=1}^{N^1} k_p j \tanh k_p j (x - v_p t - x_p); \quad (3.24)$$

by setting $u = u_s + u$ and $' = ' _s + '$, we obtain the coupled linear equations of motion

$$\frac{\partial}{\partial t} u_s r' u = r'^2 ' + (r u_s) u; \quad (3.25)$$

$$\frac{\partial}{\partial t} u_s r' ' = r'^2 u + (r' _s) u; \quad (3.26)$$

determining the fluctuation spectrum of superimposed linear modes.

The analysis proceeds as in the noiseless case. Referring to Eqs. (2.21) and (3.24) we note that in the inter-soliton matching regions of constant slope and noise fields $r u_s = r' _s = 0$. The Eqs. (3.25) and (3.26) then decouple as in the linear Edwards-Wilkinson case and setting $u_s = u$ and looking for solutions of the plane wave form $u; ' / \exp(-E_k t) \exp(ikx)$ we obtain $u ' / \exp(-E_k t) \exp(ikx)$, i.e., $u / [A \exp(-E_k^+ t) + B \exp(-E_k^- t)] \exp(ikx)$, where the non-Hermitian complex eigenvalue spectrum similar to the noiseless case is given by

$$E_k = k^2 - ivk; v = u; \quad (3.27)$$

The u mode (and likewise the $'$ mode) thus corresponds to a propagating wave with both a growing and decaying component,

$$u / (A e^{-k^2 t} + B e^{k^2 t}) e^{ik(x+vt)}; \quad (3.28)$$

These aspects are consistent with the general phase space behavior depicted in Fig. 2, whereas the propagating aspect as in the noiseless case is the manifestation of a mode transmutation from diffusive modes in the Edwards-Wilkinson case to propagating modes in the Burgers case. As indicated in Fig. 4 the linear mode propagates to the left for $u > 0$ and to the right for $u < 0$; for $u = 0$ the propagation velocity vanishes and we retrieve the diffusive modes in the Edwards-Wilkinson case. We note in particular that for a static right hand soliton with boundary values $u = u$, equivalent to the noiseless case discussed above, the mode propagates towards the soliton center which acts like a sink; for a static noise-induced left hand soliton with boundary values $u = -u$ the situation is reversed and the modes propagate away from the soliton which in this case plays the role of a source.

In the soliton regions the slope and noise fields vary over a scale k_s^{-1} and we must address the equations (3.25) and (3.26). Introducing the auxiliary variables

$$X = u ' ; \quad (3.29)$$

and the general gauge function g_s defined by the slope profile

$$g_s(x;t) = \frac{1}{2}u_s(x;t); \quad (3.30)$$

the equations (3.25) and (3.26) take the form

$$\frac{\partial X}{\partial t} = D(g_s)X - \frac{1}{2}(ru_s - r'_s)X; \quad (3.31)$$

where $D(g_s)$ is the "gauged" Schrodinger operator

$$D(g_s) = (r - g_s)^2 + \frac{1}{4}u_s^2 - \frac{1}{2}r'_s; \quad (3.32)$$

describing the motion of a particle in the soliton-defined potential $(\frac{1}{2}=4)u_s^2 - (\frac{1}{2})r'_s$ subject to the gauge field g_s . In the regions of constant slope and noise fields we have $ru_s = r'_s = 0$, $u_s = u$, $g_s = u/2$, $D(g_s) = (r - u/2)^2 + (\frac{1}{2}=4)u^2$, and searching for solutions of the form $X = \exp(-E_k t) \exp(ikx)$ we recover the spectrum in Eq. (3.27) and since $u = X^+ + X^-$ the mode in Eq. (3.28). In the soliton regions we have $r'_s = ru_s$, where $= 1$ for the right and left hand solitons, respectively, and one of the equations (3.32) decouple driving the other equation parametrically.

The analysis proceeds in a manner analogous to the noiseless case. Introducing the Cole-Hopf transformation

$$U(x;t) = \exp \int_{x_0}^x g_s(x^0;t) dx^0; \quad (3.33)$$

and using the identity $(r + g_s)^2 = U r^2 U^{-1}$ we arrive at the coupled Hermitian equations

$$\frac{\partial X}{\partial t} = U^{-1} D(0) U^{-1} X - \frac{1}{2}(ru_s - r'_s)X; \quad (3.34)$$

which are readily analyzed in terms of the spectrum of $D(0)$ summarized in Eqs (3.11) to (3.15). The exponent or generator in the gauge transformation in Eq. (3.33) samples the area under the slope profile u_s up to the point x . For $x \rightarrow 1$, $U \rightarrow \exp(-M/2)$, where M given by Eq. (1.17) is the conserved total area. In terms of the height field h , $u = rh$, $M = h(+L) - h(-L)$ for a finite system and thus equal to the height offset across a system of size L , i.e., a conserved quantity under growth. Inserting the soliton profile u_s in Eq. (2.21) the transformation U factorizes in contributions from the individual local solitons, i.e.,

$$U(x;t) = \prod_{p=1}^N U_p(x;t)^{\text{sign}(k_p)}; \quad U_p(x;t) = \cosh^{-1} k_p (x - v_p t - x_p); \quad (3.35)$$

1. The single soliton case

Since the formulation of the linear mode problem in terms of Eqs. (3.25) and (3.26) deriving from the field equations (3.21) and (3.22) and yielding Eqs. (3.34) is entirely Galilean invariant, we can in analyzing the p -th single soliton segment of the multi-soliton configuration in Eq. (2.21) without loss of generality boost the soliton to a rest frame with zero velocity. Thus shifting the slope field of the p -th soliton by the amount $(u_{p+1} + u_p)$ corresponding to the propagation velocity $v_p = (\neq 2)(u_{p+1} + u_p)$, and assuming for convenience that $x_p = 0$ the soliton profile is given by u_s in Eq. (1.8). Hence we obtain $r'_s = r u_s$ and $D(0)$ given by Eq. (3.32). Noting that $U = U_p$ and $r u_s = u k_s U_p^2$ we find for the fluctuations

$$\tilde{X} = U_p X; \quad U_p = \cosh^{-1} k_s x; \quad (3.36)$$

the Hermitian mode equations

$$\frac{\partial \tilde{X}}{\partial t} = D(0) \tilde{X} - k_s^2 (\neq 1) \tilde{X}; \quad (3.37)$$

which decouple and are readily analyzed by expanding \tilde{X} on the eigenstates of $D(0)$. We obtain

$$X = \frac{2 k_s^2 A_0^{(\neq)} t + B_0^{(\neq)}}{\cosh^2 k_s x} + (A_k^{(\neq)} e^{-k_s t} + B_k^{(\neq)} e^{k_s t}) \frac{e^{ik_s x} s_k(x)}{\cosh k_s x}; \quad (3.38)$$

$$X = A_0^{(\neq)} + B_k^{(\neq)} \frac{k}{k_s^2} e^{-k_s t} e^{ik_s x} s_k(x) \cosh k_s x; \quad (3.39)$$

describing the fluctuations of the slope and noise fields $u = (X^+ + X^-)/2$ and $r' = (X^+ - X^-)/2$ or $p = X$ about the static right hand ($\neq = +1$) and left hand ($\neq = -1$) solitons. $A_0^{(\neq)}, B_0^{(\neq)}, A_k^{(\neq)}$, and $B_k^{(\neq)}$ are integration constants fixed by the initial conditions.

The first terms in Eqs. (3.38) and (3.39) are associated with the soliton translation modes $X_{TM} / r u_s / \cosh^2 k_s x$ which propagate with constant momentum X_{TM} / A_0 ; we note that the soliton position and soliton momentum are canonically conjugate variables. The envelope modulated plane wave terms in Eqs. (3.38) and (3.39) represent the fluctuations about the soliton. Since the s -matrix $s_k(x) \neq (k + ik_s)/(k - ik_s) = \exp(i k_s x)$, $k_s = 2 \tan^{-1}(k_s/k)$ for $x \neq 1$ the soliton induced potentials are transparent and the fluctuations pass through the soliton only subject to the phase shift k_s and a spatial modulation. We also

note that Levinson's theorem implies that the band is depleted by one mode corresponding to the translation mode [55].

Confining the fluctuations to the noiseless transient submanifold $p = 0$ we have $p = 0$, i.e., $u = u'$, and we obtain for the right hand soliton ($\ell = +1$) $X^- = 0$ implying $A_0^{(1)} = 0$ and $B_k^{(1)} = 0$ and thus

$$X^+ = 2u = \frac{B_0^{(1)}}{\cosh^2 k_s x} + \frac{A_k^{(1)} e^{-k_s t} e^{ik_s x} S_k(x)}{\cosh k_s x}; \quad (3.40)$$

in accordance with Eq. (3.16) in the noiseless Burgers case, i.e., a translation mode and a band of damped localized pinned modes.

Likewise, on the noisy stationary submanifold $p = 2u$ we require $p = 2u$, i.e., $u = u'$, and we obtain for the noise induced left hand soliton ($\ell = -1$) $X^+ = 0$ entailing $A^{(-)} = 0$ and $B_k^{(-)} = 0$ and we have

$$X^- = 2u = \frac{B_0^{(-1)}}{\cosh^2 k_s x} + \frac{A_k^{(-1)} e^{-k_s t} e^{ik_s x} S_k(x)}{\cosh k_s x}; \quad (3.41)$$

composed of a translation mode and localized modes. However, unlike the fluctuations about the noiseless right hand soliton which are damped, the fluctuations associated with the noisy left hand soliton are growing in time. This behavior is consistent with the phase space plot in Fig. 2 and the Edwards-Wilkinson case discussed in Sec. II.

In general there are also fluctuations perpendicular to the submanifolds and we are led to consider the coupled equations (3.38) and (3.39). The fluctuations are modulated by the gauge factors $\cosh k_s x$ and $\cosh^{-1} k_s x$. As in the noiseless case the spatial modulation of the plane wave form allows us to extend the spectrum by an analytical continuation in the wavenumber k and in this manner match the spectrum to the inter-soliton regions. In fact, noting that X^\pm according to (3.34) decouples for $r u_s, r' u_s \neq 0$ in the inter-soliton regions, we obtain by setting $k \rightarrow k - ik_s$ the shift $k = (k^2 + \frac{2}{s}) \rightarrow (k^2 - 2ik_s)$ and $\exp(ikx) \cosh^{-1} k_s x \rightarrow \text{const.}$ and we achieve a matching to the extended propagating modes. The gauge transformation in Eq. (3.35) thus permits a complete analysis of the linear fluctuation spectrum about a multi-soliton configuration.

2. The two-soliton case

In order to illustrate how the fluctuation spectrum is established across the soliton configuration and how the matching is implemented we consider the fluctuations about the

two-soliton configuration in Eq. (2.29) with associated noise field

$$\psi_2(x;t) = \frac{1}{2} \tanh \frac{k_s}{2} (x - vt - x_1) + \tanh \frac{k_s}{2} (x - vt - x_2) : \quad (3.42)$$

The Hermitian linear mode equations are given by (3.34) with $u_s = u_2$, $\psi_s = \psi_2$ and the Cole-Hopf transformation

$$U_2(x;t) = \exp \left[\frac{1}{2} \int_{x_0}^x u_2(x';t) dx' \right] : \quad (3.43)$$

The soliton pair propagates with velocity $v = u_2$ so in order to render the gauge transformation time independent and thus facilitate the analysis we boost the configuration to a rest frame, $u_2 \rightarrow u_2 - u_2 = 0$. Inserting u_2 we then obtain the specific gauge transformation

$$U_2(x) = \frac{\cosh \frac{k_s}{2} (x - x_2)}{\cosh \frac{k_s}{2} (x - x_1)} e^{k_s x/2}; \quad (3.44)$$

a special case of (3.35).

In order to simplify the discussion of the mode equations (3.34) with $D(0)$ given by (3.32) we introduce the notation $u = (u_2) \tanh k_s/2 (x - x_1)$, $x_+ = x_1$, $x_- = x_2$, for the individual solitons contributing to u_2 and ψ_2 , i.e., $u_2 = u^1 - u^2$, $u_2 = u^1 + u^2$. A simple estimate of the potential $(-2)u_2^2 = (-2)r\psi_2$ in (3.32) then yields $(k_s/2)^2 [1 - V_+ - V_-]$, where we have also introduced the notation $V = 2 \cosh^2(k_s/2)(x - x_1)$, for the soliton-induced potentials. Moreover, $(-2)(r u_2 - r \psi_2) = (k_s/2)V$, and we arrive at the two-soliton mode equations

$$\frac{\partial X}{\partial t} = U_2^{-1} D(0) U_2^{-1} X - (k_s/2)^2 V X; \quad (3.45)$$

with $D(0)$ given by

$$D(0) = -r^2 + (k_s/2)^2 (1 - V_+ - V_-): \quad (3.46)$$

In the regions of constant slope field $V = 0$ and X decouple. To the right of the soliton pair for $x > x_1; x_2$ we have $U_2 \sim \exp(k_s(x_1 - x_2)/2) \exp(k_s x/2)$ and we obtain the envelope solutions $X \sim \exp[-(k^2 + (k_s/2)^2)t] U_2^{-1} \exp(ikx)$ which are matched to the asymptotic plane wave solution by setting $k \rightarrow k - ik_s/2$, yielding $X \sim \exp(-k^2 t) \exp(ik(x - k_s t))$, i.e., a mode propagating to the right with velocity $k_s = u_2 = v$. To the left for $x < x_1; x_2$, we have $U_2 \sim \exp(k_s(x_2 - x_1)/2) \exp(k_s x/2)$ and correspondingly the envelope solutions

$X \sim \exp[-(k^2 + (k_s=2)^2)t]U_2^{-1} \exp(ikx)$. Matching these solutions to the plane wave solutions by the analytic continuation $k \rightarrow k - ik_s=2$, we obtain the same result as above. We note that the change in U_2 across the pair is given by $\exp(-k_s(x_2 - x_1)) = \exp(-(=2)u(x_2 - x_1)) = \exp(-(=2)M_2)$, where M_2 is the area enclosed by the soliton pair. In the region between the solitons for $x_1 < x < x_2$, $U_2 = \exp(k_s(x_1 + x_2)=2) \exp(-k_s x=2)$ or for $k \rightarrow k - ik_s=2$ the modes $X \sim \exp(-k^2 t) \exp(ik(x + k_s t))$, corresponding to propagation to the left with velocity $k_s = u=2 = v$. In the soliton region near x_1 we have $V = 0$. Ignoring the translation mode and phase shift effects we thus have from (3.45) $X \sim \exp(-(k^2 + (k_s=2)^2)t)U_2^{-1} \exp(ikx)$. By insertion in Eq. (3.45) we note that $V_1 U_2^{-1} = V_2 \exp(-k_s x=2) = 0$ and that X^+ thus is decoupled from X^- , yielding the solution $X^+ \sim \exp(-(k^2 + (k_s=2)^2)t)U_2 \exp(ikx)$. A similar analysis applies in the soliton region near x_2 .

For the plane wave components alone we then obtain, interpolating to the whole axis and incorporating the smatrices according to Eq. (3.15),

$$X^+ = e^{-(k^2 + (k_s=2)^2)t} \frac{\cosh(k_s=2)(x - x_2)}{\cosh(k_s=2)(x - x_1)} e^{k_s x=2} e^{ikx} S_k(x - x_1) S_k(x - x_2); \quad (3.47)$$

$$X^- = e^{-(k^2 + (k_s=2)^2)t} \frac{\cosh(k_s=2)(x - x_1)}{\cosh(k_s=2)(x - x_2)} e^{-k_s x=2} e^{ikx} S_k(x - x_1) S_k(x - x_2); \quad (3.48)$$

We thus we pick up the phase shift $\delta_k = 2 \tan^{-1}(k_s=k)$ across each soliton, the plane wave components are moreover spatially modulated by the gauge transformation $U_2 = \exp[-(=2) \int_{x_1}^R u_2 dx]$ sampling the area under u_2 .

Finally, we boost the mode to the velocity $v = k_s = u=2$, shift the wavenumber $k \rightarrow k - ik_s=2$ for X^- and obtain the modulated plane wave associated with the propagating two-soliton mode with vanishing boundary conditions

$$X^+ = e^{-k^2 t} \frac{\cosh(k_s=2)(x - vt - \frac{x}{2})}{\cosh(k_s=2)(x - vt - \frac{x}{2})} e^{ikx} S_{k+ik_s=2}(x - vt - \frac{x}{2}) S_{k-ik_s=2}(x - vt - \frac{x}{2}); \quad (3.49)$$

$$X^- = e^{-k^2 t} \frac{\cosh(k_s=2)(x - vt - \frac{x}{2})}{\cosh(k_s=2)(x - vt - \frac{x}{2})} e^{ikx} S_{k-ik_s=2}(x - vt - \frac{x}{2}) S_{k+ik_s=2}(x - vt - \frac{x}{2}); \quad (3.50)$$

The interpretation of this result is straightforward. In the regions away from the pair-soliton we obtain plane wave modes with both a growing and decaying time behavior. Across the propagating two-soliton configuration the plane wave amplitude and form is modified by the gauge factor and the smatrix.

3. The multi-soliton case

In the multi-soliton case the slope configuration u_s and the associated noise field r'_s are given by Eqs. (2.21) and (3.24). The linear mode problem is defined by Eqs. (3.34) with the gauge transformation U given by Eq. (3.33). As discussed previously the extended plane wave modes in the inter-soliton regions connecting the solitons are subject to a mode transmutation to propagating waves with spectrum given by Eqs. (3.27). In the soliton regions the analysis follows from a generalization of the single and two-soliton cases discussed above.

A complete analysis is achieved by first noting that U also can be expressed in the form

$$U(x;t) = \exp \left[\frac{i}{2} \int_{t^0}^t dt \left(-\frac{1}{2} u_s^2(x;t^0) + r'_s(x;t^0) \right) \right]; \quad (3.51)$$

derived by differentiating U in Eq. (3.33), using the equation of motion in Eq. (3.21) for the multi-soliton profile and solving the ensuing differential equation. By insertion of Eq. (3.51) in Eqs. (3.34) we obtain the linear equations of motion

$$\frac{\partial}{\partial t} U^{-1} X = (r^2 + r'_s) U^{-1} X + \frac{1}{2} (r u_s - r'_s) U^{-1} X; \quad (3.52)$$

which are readily discussed. In the flat regions $r u_s = r'_s = 0$, X^+ and X^- decouple and we have

$$X^\pm = e^{ik^2 t} e^{ikx} U^{-1}(x;t); \quad (3.53)$$

describing a plane wave mode modulated across the soliton regions by the Cole-Hopf transformation $U(x;t)$ with the explicit form given by Eq. (3.35). Alternatively, we obtain a mode transmutation to a propagating plane wave between solitons by the analytical continuation $k \rightarrow k - ik_s$ thus absorbing the spatial modulation in $U(x;t)$ and corroborating the previous discussion. We note that the form in Eq. (3.53) is in accordance with Eqs. (3.49) and (3.50) in the two-soliton case. Across the soliton regions X^+ and X^- couple according to Eqs. (3.52). The analysis in the single soliton case above applies and the plane wave mode picks up the phase shift k_s associated by Levinson's theorem with the formation of the soliton translation modes.

IV . STATISTICAL PROPERTIES - CORRELATIONS - SCALING

In this section we discuss the statistical properties of a growing interface on the basis of the canonical phase space formulation. Generally, we can express the noisy Burgers equation in Eq. (1.1) in the form

$$\frac{\partial u}{\partial t} = -r \frac{F}{u} + u r u + r ; \quad (4.1)$$

where the free energy F driving the diffusive term is given by

$$F = \frac{1}{2} \int dx u^2(x); \quad (4.2)$$

For $r = 0$ we have the linear Edwards-Wilkinson equation describing the temporal fluctuations in a thermodynamic equilibrium state with temperature $T = \beta^{-1} k_B$ with stationary distribution given by Eq. (1.21), i.e., $P_{st} \propto \exp[-F/k_B T]$. In the presence of the nonlinear mode coupling term $u r u$ Eq. (4.1) does not describe a thermodynamic equilibrium state but a stationary nonequilibrium state or kinetic growth state. It is, however, a particular feature of the one dimensional case that the stationary distribution is known and given by $P_{st} \propto \exp[-F/k_B T]$, independent of r . This property also follows from the potential condition [46, 47, 49]

$$\int dx \left[r u - \frac{F}{u} r(u^2) \right] = 0; \quad (4.3)$$

which is readily satisfied since the integrand becomes a total derivative. Another way of noting that Eq. (4.1) does not describe an equilibrium state is to express the equation in the form $\partial u / \partial t = -r F' / u + r$ with effective free energy $F' = (1/2) \int dx (u^2 + (1/3) u^3)$. Apart from the fact that F' includes an odd power in u and thus, since $u = r h$, violates parity invariance it is also unbounded from below for $u \rightarrow -\infty$ and thus cannot describe a stable thermodynamic state.

The stationary distribution $P_{st}(u)$ is obtained in the limit $t \rightarrow \infty$ from the transition probability $P(u^i \rightarrow u; t)$ for a pathway from the initial configuration u^i to the final configuration u . In this limit only the linear diffusive modes for $r = 0$ persist characterized by P_{st} . This is consistent with the fact that the soliton contribution yields $P(u^i \rightarrow u; t) \propto \exp[-S(t)]$, where the action $S(t)$ associated with the solitonic growth modes, e.g., the two-soliton configuration, typically grows linearly with t implying that the contribution to P vanishes.

A . Correlations in the Edwards-W ilkinson case

In the linear case the correlation function is easily evaluated on the Langevin level from the stochastic Edwards-W ilkinson equation (2.2) and follows directly from Eq. (2.1) when averaging over the noise, see also paper II. In wavenumber-frequency space we obtain the Lorentzian dispersive form

$$\text{huui}(\mathbf{k};!) = \frac{k^2}{!^2 + (k^2)^2}; \quad (4.4)$$

with dispersive poles at $! = \pm i k^2$, strength $= (k^2)^2$ and linewidth k^2 . We note that both growing, $u / \exp(-k^2 t)$, and decaying terms, $u / \exp(-k^2 t)$, contribute to the stationary correlations; this is in accordance with the decomposition (2.14). In wavenumber-time space we have correspondingly

$$\text{huui}(\mathbf{k};t) = \frac{1}{2} e^{-k^2 |t|}; \quad (4.5)$$

and the dispersive correlations decay on a time scale determined by $1/k^2$. For the equal-time correlations we obtain in particular $\text{huui}(\mathbf{k};0) = 1/2$, showing the spatially short ranged correlations in accordance with the stationary distribution (1.21). For later purposes we also need the spectral form, see paper II,

$$\text{huui}(\mathbf{x};t) = \frac{1}{2} \int \frac{d\mathbf{k}}{2\pi} e^{i\mathbf{k}\cdot\mathbf{x}} e^{-k^2 |t|}; \quad (4.6)$$

In order to illustrate the method to be used later in the soliton case we evaluate here huui in the linear case on the basis of the path integral formulation Eq. (1.14). Since that the distributions (1.21) and (2.13) factorize in wavenumber space we have in a little detail for a system of size L

$$\text{huui}(\mathbf{k};t) / \int \prod_p du_p^f du_p^i u_k^f u_k^i \exp \left[-\frac{1}{L} \sum_n \frac{u_n^f u_n^i}{1 - e^{-2|t|}} \right] \exp \left[-\frac{1}{L} \sum_m j_m^i j_m^f \right]; \quad (4.7)$$

Changing variables in $P(u_n^f; u_n^i; t)$, $u_n^f = u_n^i \exp(-|t|)$, it is an easy task to carry out the Gaussian integrals over u_n and u_n^i and retrieve $\text{huui}(\mathbf{k};t)$ in Eq. (4.5); the evaluation of huui in the corresponding harmonic oscillator quantum field calculation was performed in paper II. Finally, evaluating Eq. (4.6) we infer the scaling form (1.20) with roughness exponent $= 1/2$, dynamic exponent $z = 2$, and scaling function, see also paper II,

$$\tilde{F}(w) = \frac{1}{2} [4]^{-1/2} w^{-1/2} e^{-1/4 w}; w = t x^z; \quad (4.8)$$

defining the Edwards-Wilkinson universality class.

Summarizing, the Edwards-Wilkinson equation describes a thermodynamic equilibrium state. The dynamical equilibrium fluctuations are characterized by the gapless dispersion law $\omega = k^2$. The modes are extensive and diffusive and controlled by the characteristic decay time $\tau = k^{-2}$, depending on the wavenumber k .

B. Switching and pathways in the Burgers-KPZ case

Before we turn to the correlations in the nonlinear Burgers-KPZ case it is instructive to extract a couple of simple qualitative consequences of the dynamical approach. As discussed in Sec. II the propagation of a two-soliton configuration constitutes a simple growth situation where at each passage of the soliton pair the interface grows by a layer. Considering a pair configuration of amplitude u and size ℓ the propagation velocity is $v = u/2$ and the associated action $S_1 = (1/6) \int_0^T \ell^3 dt$. Across a system of size L we have $\ell T = L$, where T is the switching time, i.e., $\ell = 2L/T$. For the action associated with the transition pathway of adding a layer of thickness $h = \int_0^T u(x^0; t) dt = \ell T = 2L$ we then have

$$S_1(T) = \frac{4}{3} \frac{L^3}{T^2} : \quad (4.9)$$

We note that the thickness h does also depend on the pair-soliton size ℓ which does not enter in the action. However, the multiplicity or density of soliton pair which enters in the prefactor of the transition probability must depend on ℓ and we obtain qualitatively

$$P \propto \ell^{-1} \exp \left[-\frac{4}{3} \frac{L^3}{T^2} \right] : \quad (4.10)$$

In the thermodynamic limit $L \rightarrow \infty$, $P \rightarrow 0$ and the switching via a two-soliton pathway is suppressed. At long times the action falls off as ℓ^{-2} .

In the case of a switching pathway by means of two equal amplitude pair-solitons we obtain, correspondingly, noting that the pairs propagate with half the velocity, the action $S_2 = (1/4)S_1$. Introducing heuristically a constant nucleation action S_{nuc} associated with the noise-induced formation of a pair, i.e., the appropriate assignment of the noise field p , we have the general expression for the action associated with n pairs

$$S_n(T) = nS_{\text{nuc}} + \frac{1}{n^2} \frac{4}{3} \frac{L^3}{T^2} : \quad (4.11)$$

In Fig. 10 we have plotted S versus T for $n = 1 \dots 5$ soliton pairs. Since the curves intersect we infer that the switching at long times takes place via a single soliton pair. At shorter times a switching takes place and the transition pathway proceeds by the excitation of multipair-solitons. This is clearly a finite size effect.

A similar analysis of the soliton switching pathways in the case of the noise driven Ginzburg-Landau equation has recently been carried out. Here the analysis, corroborating recent numerical optimization studies, is simpler because the soliton excitations are topological and have a fixed amplitude [59].

C. Anomalous diffusion of growth modes in the Burgers-KPZ case

On the Langevin level the growth of the interface is a stochastic phenomena driven by noise. Parameterizing the growth in terms of growth modes corresponding to the propagation of a gas of independent pair-solitons in the slope field the dynamical approach allows a simple interpretation. Noting that the action associated with the pair mode is given by $S = (1/6) \int u^3 dx$ and denoting the center of mass of the pair mode by $x = (x_1 + x_2)/2$ we have $u = 2v = 2x/t$ and we obtain the transition probability

$$P(x;t) \propto \exp \left(-\frac{4}{3} \frac{x^3}{t^2} \right); \quad (4.12)$$

for the random walk of independent pair-solitons or steps in the height profile. Comparing (4.12) with the distribution for ordinary random walk originating from the Langevin equation $dx/dt = \eta$; $\langle x^2(t) \rangle = 2t$, $P(x;t) \propto \exp(-x^2/2t)$, we conclude that the growth mode performs anomalous diffusion. Assuming pairs of the same average size, the distribution (4.12) also implies the soliton mean square displacement,

$$\langle x^2(t) \rangle \propto t^{1-z}; \quad (4.13)$$

with dynamic exponent $z = 3/2$, identical to the dynamic exponent defining the KPZ universality class. This result should be contrasted with the mean square displacement $\langle x^2(t) \rangle \propto t^{2-z}$, $z = 2$, for ordinary random walk. The growth modes thus perform superdiffusion. This result is also obtained using the mapping of the KPZ equation to directed polymers in a random medium [22].

The diffusion of solitons or growth modes is another signature of the stationary nonequilibrium state. Whereas the extended diffusive equilibrium modes for a particular wavenumber k are characterized by the stationary distribution $P_{st} \propto \exp(-(\epsilon/L)j_k^2)$, the random walk distribution of the growth modes $P(x;t) \propto t^{-2/3} \exp(-x^3/t^2)$ vanishes for $t \rightarrow 1$. The growth modes or solitons disperse diffusively over the system and generate the stationary growth.

D. Correlations in the Burgers-KPZ case – general

As regard the correlations in the nonlinear Burgers-KPZ case the situation is more complex. The noisy Burgers equation (1.1) is not easily amenable to a direct analysis of the noise averaged correlations and we limit ourselves to a discussion of $hu_i(x;t)$ within the canonical phase space approach. In order to evaluate the slope correlations $hu_i(x;t)$ by means of Eq. (1.14), i.e.,

$$hu_i(x;t) = \int du^i du^f u^f(x) u^i(0) P(u^f; u^i; t) P_{st}(u^i); \quad (4.14)$$

we note that the basic ingredient is the transition probability $P(u^f; u^i; t)$ from an initial configuration u^i at time $t=0$ to a final configuration u^f at time t .

1. Sum rule

Before continuing we observe that in the short time limit $t \rightarrow 0$ it follows from the definition that $P(u^f; u^i; t) \rightarrow \delta(u^f - u^i)$. The equal time correlations are thus determined by the stationary distribution $P_{st}(u^i)$ given by Eq. (1.21),

$$P_{st}(u^i) \propto \exp \left(- \int dx u^i(x)^2 \right); \quad (4.15)$$

and we have in wavenumber space $hu_i(k;0) = -2$. In wavenumber-frequency space we thus infer the general sum rule

$$\frac{d}{d\omega} hu_i(k; \omega) = \frac{1}{2}; \quad (4.16)$$

The sum rule is independent of the presence of the nonlinear growth term $u \partial_x u$ and thus is another consequence of the static fluctuation dissipation theorem which holds for the Burgers-KPZ equations [22, 36].

2. The transition probability

As discussed in Sec. II the working hypothesis is that a growing interface at a particular time instant can be represented by a dilute gas of matched localized soliton excitations or growth modes with superimposed linear extended diffusive modes. From the analysis in Sec. III we thus have

$$u(x;t) = u_s(x;t) + u_l(x;t); \quad (4.17)$$

$$p(x;t) = p_s(x;t) + p_l(x;t); \quad (4.18)$$

where u_s and p_s (or u'_s) are given by the multi-soliton representations in Eqs. (2.21) and (2.22) (or for u'_s in Eq. (3.24)). In the flat regions for constant slope $u = (1/2)(X^+ + X^-)$ and $p = X^-$ are given by Eqs. (3.53) (across the soliton regions u and p vary in a more complicated manner as discussed in Sec. III).

Inserting Eqs. (4.17) and (4.18) in Eq. (1.10) and using the equation of motion (1.6) the action S decomposes in a soliton contribution S_{sol} and a linear contribution S_{lin} , $S = S_{sol} + S_{lin}$, where

$$S_{sol} = \frac{1}{2} \int^Z dx dt (r p_s)^2; \quad (4.19)$$

$$S_{lin} = \frac{1}{2} \int^Z dx dt (r p)^2; \quad (4.20)$$

This decomposition implies that the transition probability $P(u^f; u^i; t)$ accordingly factorizes like

$$P(u^f; u^i; t) = P_{sol}(u_s^f; u_s^i; t) P_{lin}(u^f; u^i; t); \quad (4.21)$$

where $P_{sol} / \exp(-S_{sol})$ and $P_{lin} / \exp(-S_{lin})$. Disregarding phase shift effects and amplitude modulations due to the dilute soliton gas, P_{lin} can be worked out as in the Edwards-Wilkinson case in Sec. II, yielding the expression (in wavenumber space)

$$P(u^i; u^f; t) / \exp(-S_{lin}) = \frac{1}{2} \int^Z \frac{dk}{2\pi} \frac{u_k^f \exp(-ik t)}{u_k^i \exp(-ik t)}; \quad (4.22)$$

with limiting distribution $P_{st}(u^f) / \exp(-S_{lin}) = \int^R (dk/2\pi) u_k^f$ for $t \rightarrow \infty$.

For the soliton part we obtain inserting Eq. (2.26)

$$P(u^i; u^f; t) / \exp(-S_{sol}) = \frac{1}{6} \int^Z \frac{dk}{2\pi} \frac{u_k^f \exp(-ik t)}{u_k^i \exp(-ik t)}; \quad (4.23)$$

in terms of the soliton boundary values u_p as depicted in Fig. 4. Note also that only the noise induced left hand solitons contribute to the action. We stress that the expression (4.23) by construction only holds in-between soliton collisions. In fact, at long times the appropriate expression for $P(u^i; u^f; t)$ must approach $P_{st} / \exp[-(\sum_{p \in p^0}^R dx u_s^f(x))^2]$ in accordance with Eq. (4.21). Likewise, the correct expression for the multi-soliton energy must vanish in the long time limit corresponding to the migration of the phase space orbit to the transient and stationary zero energy submanifolds $p = 0$ and $p = 2u$, as discussed in paper III.

3. Multi-soliton correlations - Scaling properties

Inserting Eq. (4.17) in Eq. (4.14) the slope correlations separate in a soliton part and a linear (diffusive) part,

$$h u u i(x; t) = h u_s u_s i(x; t) + h u u i(x; t); \quad (4.24)$$

Apart from phase shift and amplitude modulation effects due to the dilute soliton gas, the linear or diffusive correlations $h u u i$ basically have the form given by Eq. (4.6). For the soliton contribution $h u_s u_s i$ we obtain, inserting u_s from Eq. (2.21), $P(u_s^f; u_s^i; t)$ from Eq. (4.23), and for the stationary distribution

$$P_{st} / \exp^4 \left[- \sum_{p=1}^N u_p^2 j_p \right] \sum_{p \in p^0}^3 x = \exp^4 \left[- \frac{8}{2} \sum_{p \in p^0}^3 x k_p k_{p^0} j_p \right] \sum_{p \in p^0}^3 x; \quad (4.25)$$

and moreover introducing the soliton amplitude $k_p = (\sum_{p=1}^4) (u_{p+1} - u_p)$ from Eq. (2.19),

$$h u_s u_s i(x; t) = \sum_{p \in p^0}^N \int_{-L}^L dx_1 dv_1 dx_1 k_p k_q \tanh j_p j(x_p + v_p t - x) \tanh j_q j_q \exp \left[- \frac{32}{3} t j_n^3 \left(\sum_{n \in n^0}^Y k_n \right) \right] \sum_{n \in n^0}^Y \exp \left[- \frac{8}{2} k_n k_{n^0} (x_n - x_{n^0}) \right]; \quad (4.26)$$

This formula expresses the contribution to the slope correlations from a multi-soliton configuration. It follows from the derivation that the expression only holds for times short compared to the soliton collision time. The initial configuration u_s^i at time $t = 0$ propagates during time t to the final configuration u_s^f . The associated transition probability is given by Eq. (4.23) and the stationary distribution by Eq. (4.25). The integration over initial and final configurations is effected by integrating over the amplitudes k_p , the velocities v_p and the soliton positions x_p over a system of size L . Note that k_p together with

$v_p = (\pm 2)(u_{p+1} + u_p)$ determine the slope u_p . Likewise the dynamic partition function $Z(t)$ is given by

$$Z(t) = \int \prod_{n \in \mathbb{Z}} dk_n dv_n dx_n \exp \left[-\frac{32}{3} t \sum_{n \in \mathbb{Z}} k_n^3 \right] \left(\prod_{n \in \mathbb{Z}} \int dx_n \exp \left[-\frac{8}{2} k_n k_{n^0} (x_n - x_{n^0}) \right] \right) : (4.27)$$

The complex form of Eqs. (4.26) and (4.27) have so far precluded a more detailed analysis. We can, however, in the limit of small damping extract the general scaling properties. For $\gamma \rightarrow 0$ we have $k_p \rightarrow 1$ and the soliton profile given by $\tanh[k_p(x - v_p t - x_p)]$ converges to the sign function $\text{sgn}(x - v_p t - x_p)$, corresponding to a sharp shock wave. By inspection of Eq. (4.26) we note that a change of the length scale by a factor λ , i.e., $x \rightarrow \lambda x$ and $x_p \rightarrow \lambda x_p$, can be absorbed by a change of the integration variable k_p , $k_p \rightarrow \lambda^{-1} k_p$. In the action term this change of k_p is naturally absorbed by the scale transformation $t \rightarrow \lambda^3 t$. Consequently, for $\gamma \rightarrow 0$ we have $h_{uu}(x;t) = F(t=x^{3/2})$ in accordance with the general scaling form in Eq. (1.20).

E. Correlations in the Burgers-KPZ case – the two-soliton sector

In the weak noise limit $\gamma \rightarrow 0$ the action in Eq. (1.11) provides a general selection criterion determining the dominant dynamical configuration contributing to the distribution P . In the present section we propose that part of the leading growth morphology is constituted by a gas of two-soliton or pair configurations already analyzed in Sec. II. In our numerical studies we have demonstrated that in the limit $\gamma \rightarrow 0$ the pair configuration does constitute a long lived quasi-particle [39].

The evaluation of the contribution to the slope correlations from the two-soliton sector is straightforward and will permit a more detailed scaling analysis. Specializing the general expression in Eqs. (4.26) and (4.27) to the case of two solitons, i.e., a pair-soliton excitation, noting that $k_1 = -k_2 = (\pm 4)u$, $u_2 = u$ ($u_1 = u_3 = 0$), and $v_1 = v_2 = v = (\pm 2)u$, and moreover considering the limit of small γ , or, alternatively, using the expressions pertaining to the two-soliton case discussed in Sec. II, we have

$$h_{uu}(x;t) \xrightarrow{\gamma \rightarrow 0} \frac{1}{4} \int dx_1 dx_2 u^2 [\text{sign}(x_1) - \text{sign}(x_2)] [\text{sign}(x_1 - x_2 - vt) - \text{sign}(x_2 - x_1 - vt)] \exp \left[-\frac{t}{6} \sum_{i=1}^2 k_i^3 \right] \exp \left[-u^2 \sum_{i=1}^2 k_i x_i \right]; \quad (4.28)$$

with dynamic partition function

$$Z(t) = \int_0^L dx_1 dx_2 \exp \left[-\frac{t}{6} \int_0^L dx \left(\frac{1}{2} \left(\frac{dx}{dx_1} \right)^2 + \frac{1}{2} \left(\frac{dx}{dx_2} \right)^2 \right) \right] \quad (4.29)$$

We note that the final configuration u^f is simply the initial two-soliton configuration u^i displaced vt along the axis without change of shape. This dynamical evolution is depicted in Fig. 11. The integration over initial and final configurations is carried out by integrating over the soliton amplitude u , $-1 < u < 1$ and the soliton positions x_1 and x_2 over a system of size L . The integration over the amplitude only contributes to integral when the pair-solitons overlap, as indicated in Fig. 12, and we obtain by inspection of the overlap contribution, setting $z = x_2 - vt$ and $\ell = x_2 - x_1$ the conditions $x_1 < z$, $x_1 > z - \ell$, $x_1 < 0$, and $x_1 > -\ell$. For $z > 0$, i.e., $x_2 - vt > 0$ we have the overlap conditions $0 < z < \ell$ and $z - \ell < x_1 < 0$; for $z < 0$ we obtain $-\ell < z < 0$ and $-\ell < x_1 < z$. Finally, integrating over the soliton position x_1 and the soliton pair size ℓ we arrive at the expression

$$h_{uu}(x;t) = \frac{1}{L} \frac{\int_{-1}^1 du u^2 \exp \left[-\frac{t}{6} \int_0^L dx \left(\frac{1}{2} \left(\frac{dx}{dx_1} \right)^2 + \frac{1}{2} \left(\frac{dx}{dx_2} \right)^2 \right) \right] C_L^{(1)}(u)}{\int_{-1}^1 du \exp \left[-\frac{t}{6} \int_0^L dx \left(\frac{1}{2} \left(\frac{dx}{dx_1} \right)^2 + \frac{1}{2} \left(\frac{dx}{dx_2} \right)^2 \right) \right] C_L^{(2)}(u)}; \quad (4.30)$$

where the cut-off functions $C_L^{(1)} = \int_0^L dx \exp \left(-\frac{t}{6} \int_0^L dx \left(\frac{1}{2} \left(\frac{dx}{dx_1} \right)^2 + \frac{1}{2} \left(\frac{dx}{dx_2} \right)^2 \right) \right)$ and $C_L^{(2)} = \int_0^L dx \exp \left(-\frac{t}{6} \int_0^L dx \left(\frac{1}{2} \left(\frac{dx}{dx_1} \right)^2 + \frac{1}{2} \left(\frac{dx}{dx_2} \right)^2 \right) \right)$ follow from the overlap; explicitly they are given by

$$C_L^{(1)}(u) = -\frac{1}{u^4} \left(1 - \exp \left(-\frac{u^2 L}{2} \right) \right); \quad (4.31)$$

$$C_L^{(2)}(u) = -\frac{1}{u^2} \left(1 - \exp \left(-\frac{u^2 L}{2} \right) \right); \quad (4.32)$$

The overall factor $1/L$ reflects the weight of a single pair-soliton contribution to the correlations function. In the thermodynamic limit $L \rightarrow \infty$ this contribution vanishes. For a dilute gas of pair-solitons of density n we expect $1/L$ to be replaced by n . On the other hand, the further L dependence of the cut-off functions, is a feature of the extended nature of the pair-soliton already discussed in Sec. II. Both $C^{(1)}$ and $C^{(2)}$ vanish as a function of u over a scale set by $\ell = L$. For $u \rightarrow 1$ $C^{(1)} \sim 1/u^4$ and $C^{(2)} \sim 1/u^2$; for $u = 0$ we have $C^{(1)} = L^2/2$ and $C^{(2)} = L$.

F. General scaling properties

The last issue we deal with is the scaling properties of a growing interface. The dynamical scaling hypothesis [17, 22] and general arguments based on the renormalization group fixed-

point structure [24, 25] imply the following long time - large distance form of the slope correlations in the stationary state:

$$\langle u(x;t) u(x';t) \rangle = (x-x')^{-2} F(x-x'/\ell(t)) \quad (4.33)$$

Here F is the scaling function and the roughness exponent α follows from the explicitly known stationary distribution in Eq. (1.21), the fluctuation dissipation theorem. Within the canonical phase space approach the stationary distribution follows from the structure of the zero-energy manifolds which attract the phase space orbits in the long time limit $t \rightarrow \infty$, see paper III. The dynamic exponent $z = 3/2$ is inferred from the gapless soliton dispersion law in Eq. (2.36), see paper II. Since the formulation is entirely Galilean invariant the exponent z also follows from the scaling law $\alpha + z = 2$ in Eq. (1.3).

The lateral growth of fluctuations along the interface is conveniently characterized by the time dependent correlation length $\ell(t)$. Note that for a finite system of size L the correlation length saturates at the crossover or saturation time t_{∞} determined by $\ell(t_{\infty}) = L$. In the linear Edwards-Wilkinson case $\ell(t)$ characterizes the growth of diffusive modes and has the form $\ell(t) = (t)^{1/2}$, consistent with the spectral form in Eq. (4.6). In the Burgers-KPZ case $\ell(t)$ describes the propagation of soliton modes and is given by $\ell(t) = (t)^{1/3}$. The limiting form of the scaling function $\lim_{w \rightarrow 1} F(w) = 1$ for $x \ll \ell(t)$. In the dynamical regime for $\ell(t) \ll x$ the correlation decay, i.e., $\langle u(x;t) u(x';t) \rangle \rightarrow 0$, and the scaling function vanishes like $F(w) \sim w^{-2(1-\alpha)}$ for $w \rightarrow 0$. In Fig. 13 we have depicted the correlation length $\ell(t)$ as a function of time for a system of size L , indicating the crossover behavior in the Edwards-Wilkinson and Burgers-KPZ cases. In Fig. 13 we have plotted the time scale T as a function of system size indicating the various dynamic regimes.

G. Scaling properties in the two-soliton sector

In discussing the scaling properties associated with the two-soliton sector it is convenient to introduce the model parameters ℓ_0 , setting the microscopic length scale, t_0 , setting the microscopic time scale, t_{∞} denoting the crossover or saturation time for a system of size L , and the correlation length $\ell(t)$, note that $\ell_0 = \ell_0 = t_0$,

$$\ell_0 = \ell_0; \quad (4.34)$$

$$t_0 = \frac{x}{2}; \quad (4.35)$$

$$t_{\infty} = t_0 (L=x_0)^{3=2}; \quad (4.36)$$

$$(t) = x_0 (t=t_0)^{2=3}; \quad (4.37)$$

Rescaling the amplitude variable u we can then express the pair correlations in the form

$$h_{uu}(x,t) = \frac{x_0}{L} \frac{\int_0^R du \exp \left[\frac{4}{3} j u^3 \frac{t}{t_{\infty}} \right] \exp \left[\frac{4u^2}{L} x + u \frac{t}{t_{\infty}} j F_1(u) \right]}{\int_0^R du \exp \left[\frac{4}{3} j u^3 \frac{t}{t_{\infty}} \right] F_2(u)}; \quad (4.38)$$

where the cut-off functions originating from the overlap are given by

$$F_1(u) = \frac{1}{4u^2} \left(1 + \frac{1}{4u^2} \exp(-4u^2) \right); \quad (4.39)$$

$$F_2(u) = \frac{1}{4u^2} \left(1 - \exp(-4u^2) \right); \quad (4.40)$$

The expression (4.38) holds for $t > 0$ and is even in x (seen by changing u to $-u$). It samples the soliton pair propagating with velocity $u=2$ and is in general agreement with spectral form discussed in the quantum treatment in paper II.

The weight of a single soliton pair is of order $1=L$ and the correlation function h_{uu} thus vanishes in the thermodynamic limit $L \rightarrow \infty$. For a finite system L enters setting a length scale together with the saturation time t_{∞} defining a time scale, and h_{uu} is a function of $x=L$ and $t=t_{\infty}$ as is the case for the two-soliton expression (4.38). It is instructive to compare this dependence with the wavenumber decomposition of h_{uu} in the linear dispersive case for $\nu = 0$. Here $h_{uu}(x,t) / (1=L)^P \sum_{n \neq 0} \exp(-(2n)^2 t=L^2) \exp(inx=L)$, depending on $x=L$ and $t=L^2$, corresponding to the saturation time t_{∞} / L^2 , $z = 2$. Keeping only one mode for $n = 1$ the correlations h_{uu} has the same structure as in the soliton case. In the linear case we can, of course, sum over the totality of modes and in the thermodynamic limit $L \rightarrow \infty$ replace $(1=L)^P \sum_n$ by $\int_{-\infty}^{\infty} dk=2$ obtaining the intensive correlations $h_{uu}(x,t) = (\nu=2)(4-t)^{-1=2} \exp(-x^2=2t)$. Similarly, we expect the inclusion of multi-soliton modes to allow the thermodynamic limit to be carried out yielding an intensive correlation function in the Burgers case.

For a finite system we have in general [60] $h_{uu}(x,t) = (1=L)G_L(x=L;t=L^{3=2})$ with scaling limits: $G_L(x=L;0) / \text{const.}$ for $x \ll L$, $G_L(x=L;0) / L=x$ for $x \gg L$ and $G_L(0;t=L^{3=2}) / \text{const.}$ for $t \ll L^{3=2}$, $G_L(0;t=L^{3=2}) / L=t^{2=3}$ for $t \gg L^{3=2}$. For $L \rightarrow \infty$ we obtain $G_L(x=L;t=L^{3=2}) \rightarrow (L=x)G(x=t^{2=3})$ in conformity with (4.33).

It is an important feature of the two-soliton expression (4.38) that the dynamical soliton interpretation directly implies the correct dependence on the scaling variables $x=L$ and $t=t_\infty / t=L^{3=2}$, independent of a renormalization group argument. However, the scaling limits are at variance with G_L . Setting, according to (4.38) $hu_i(xt) = (\lambda_0=L)F(x=L; t=t_\infty)$, $F(x=L; 0)$ assumes the value .47 for $x \rightarrow L$ and decreases monotonically to the value .08 for $x \rightarrow L$, whereas G_L diverges as $L=x$ for $x \rightarrow L$. Likewise, $F(0; t=t_\infty)$ decays from .47 for $t \rightarrow t_\infty / L^{3=2}$ to 0 for $t \rightarrow t_\infty$; for $t \rightarrow t_\infty$ we have $F_2 \rightarrow .15$, whereas G_L diverges as $L=t^{2=3}$ for $t \rightarrow t_\infty$.

This discrepancy from the scaling limits is a feature of the two-soliton contribution which only samples the correlation from a single soliton pair. Moreover, at long times the soliton contribution vanishes and the scaling function is determined by the dispersive mode contribution in accordance with the convergence of the phase space orbits to the stationary zero-energy manifold. We note, however, the general trend towards a divergence for small values of x and t is a feature of F .

Introducing the scaling variables $w = x = / x=t^{2=3}$ and $\tau = t=t_\infty / t=L^{3=2}$ we can also express (4.38) in the form

$$hu_i(xt) = (\lambda_0=L)F(w; \tau); \quad (4.41)$$

where the scaling function F is now given by

$$F(w; \tau) = \frac{\int_0^R du e^{\frac{4}{3}w^3} e^{-4u^2w^{2=3+u}} F_1(u)}{\int_0^R du e^{\frac{4}{3}w^3} F_2(u)}; \quad (4.42)$$

and summarize our findings in Fig. 15 where we have depicted $F(w; \tau)$ for a range of values. For fixed small $w = x = / x=t^{2=3}$ we have $F \rightarrow .47$ for $\tau = t=t_\infty / t=L^{3=2} \rightarrow 0$; for large τ we obtain $F \rightarrow 0$. The weak maximum moving towards smaller values of w for decreasing τ is a feature of the functional form of F in (4.42) and thus due to the soliton approximation. The true scaling function is not expected to have any particular distinct features [22, 24, 26, 27, 28, 29, 30, 31, 32, 33].

V. SUMMARY AND CONCLUSION

In the present paper we have continued our analysis of the noisy Burgers equation in one spatial dimension within the weak noise canonical phase space approach developed in

previous papers. We believe that the noisy Burgers equation or the equivalent KPZ equation, which have been studied intensively, is of fundamental and paradigmatic significance in the context of a continuum field theoretical description of nonlinear non equilibrium phenomena. The advantage of the canonical phase space method which is an elaboration and a dynamical system theory interpretation of the saddle point equations originating from the Martin-Siggia-Rose functional formulation or, equivalently, a phase space formulation of the Freilich-Wentzel variational approach to the Fokker-Planck equation, actually dating back to work by Machlup and Onsager [61, 62], is that it replaces the stochastic Langevin equation with coupled deterministic field equations, yielding on the one hand an interpretation of the growth morphology and pattern formation and on the other hand a practical scheme for the evaluation of the statistical properties and correlations in the weak noise limit.

Here we have in some detail discussed i) the growth morphology engendered by the propagation of domain walls or solitons, the growth modes, ii) the superimposed linear modes and their transmutation to propagating modes in the presence of the growth modes, and, finally, iii) the statical and scaling properties, particularly, in the two-soliton sector. The weak noise theory of the one dimensional Burgers or KPZ equation is, however, far from complete and many open questions remain. We mention below a series of topics which it would be of considerable interest to investigate: i) the interpretation of the soliton in growth picture in the context of the mapping of the KPZ equation to the model of directed polymers in a random medium, ii) a more complete analysis of the multi-soliton correlations in the thermodynamic limit with the purpose of making contact with other models in the KPZ universality class, e.g. the polynuclear growth model [31, 63, 64, 65], iii) elaboration of the anomalous diffusion of growth modes, iv) contact with other models for many-body systems far from equilibrium, e.g. driven lattice gas models [52], and, finally, iv) the extension of the weak noise approach to higher dimensions.

Acknowledgments

The author wishes to thank A. Svane for numerous fruitful discussions. Discussions with J. Hertz and J. Krug are also gratefully acknowledged. This work has been supported by

-
- [1] H . C . Fogedby, *Phys. Rev. E* 57, 2331 (1998).
 - [2] J. M . Burgers, *Proc. Roy. Neth. Acad. Soc.* 32, 414, 643, 818 (1929).
 - [3] J. Burgers, *The Nonlinear Diffusion Equation* (Riedel, Boston, 1974).
 - [4] H . C . Fogedby, A . B . Eriksson, and L . V . M ikheev, *Phys. Rev. Lett.* 75, 1883 (1995).
 - [5] H . C . Fogedby, *Phys. Rev. E* 57, 4943 (1998).
 - [6] P . C . M artin, E . D . Siggia, and H . A . Rose, *Phys. Rev. A* 8, 423 (1973).
 - [7] R . Baussch, H . K . Janssen, and H . W agner, *Z. Phys. B* 24, 113 (1976).
 - [8] H . K . Janssen, *Z. Phys. B* 23, 377 (1976).
 - [9] C . D . D om inicis and L . P eliti, *Phys. Rev. B* 18, 353 (1978).
 - [10] D . Forster, D . R . Nelson, and M . J . Stephen, *Phys. Rev. Lett.* 36, 867 (1976).
 - [11] D . Forster, D . R . Nelson, and M . J . Stephen, *Phys. Rev. A* 16, 732 (1977).
 - [12] H . C . Fogedby, *Phys. Rev. E* 59, 5065 (1999).
 - [13] M . I . Freidlin and A . D . W entzel, *Random Perturbations of Dynam ical System s* (2nd ed. Springer, New York, 1998).
 - [14] R . G raham , *Noise in nonlinear dynam ical system s*, Vol1, *Theory of continuous Fokker-P lanck system s*, eds. F . M oss and P . E . V . M cClintock (Cambridge University Press, Cambridge, 1989).
 - [15] H . C . Fogedby, *Phys. Rev. Lett.* 80, 1126 (1998).
 - [16] H . C . Fogedby, *Phys. Rev. E* 60, 4950 (1999).
 - [17] M . K ardar, G . Parisi, and Y . C . Zhang, *Phys. Rev. Lett.* 56, 889 (1986).
 - [18] E . M edina, T . H wa, M . K ardar, and Y . C . Zhang, *Phys. Rev. A* 39, 3053 (1989).
 - [19] P . Sa m an, *Topics in Nonlinear Physics*, ed. N . J . Zabusky (Springer, New York, 1968).
 - [20] E . Jackson, *Perspectives of nonlinear dynam ics* (Cambridge University Press, Cambridge, 1990).
 - [21] G . B . W hitham , *Nonlinear W aves* (W iley, New York, 1974).
 - [22] T . H alpin-Healy and Y . C . Zhang, *Phys. Rep.* 254, 215 (1995).
 - [23] S . F . Edwards and D . R . W ilkinson, *Proc. Roy. Soc. London A* 381, 17 (1982).
 - [24] T . H wa and E . Frey, *Phys. Rev. A* 44, R 7873 (1991).

- [25] E. Frey, U. C. Tauber, and T. Hwa, *Phys. Rev. E* 53, 4424 (1996).
- [26] U. C. Tauber and E. Frey, *Phys. Rev. E* 51, 6319 (1995).
- [27] E. Frey, U. C. Tauber, and H. K. Janssen, *Europhys. Lett* 47, 14 (1999).
- [28] M. Lässig, *Nucl. Phys. B* 448, 559 (1995).
- [29] M. Lässig, *Phys. Rev. Lett.* 80, 2366 (1998).
- [30] M. Lässig, *Phys. Rev. Lett.* 84, 2618 (2000).
- [31] M. P. rahofer and H. Spohn, *Phys. Rev. Lett.* 84, 4882 (2000).
- [32] F. Colaiori and M. A. Moore, *Phys. Rev. Lett.* 86, 3946 (2001).
- [33] F. Colaiori and M. A. Moore, *Phys. Rev. E* 63, 057103 (2001).
- [34] H. C. Fogedby, *Europhys. Lett* 56, 492 (2001).
- [35] A. L. Barabasi and H. E. Stanley, *Fractal Concepts in Surface Growth* (Cambridge University Press, Cambridge, 1995).
- [36] D. A. Huse, C. L. Henley, and D. S. Fisher, *Phys. Rev. Lett.* 55, 2924 (1985).
- [37] J. Zinn-Justin, *Quantum Field Theory and Critical Phenomena* (Oxford University Press, Oxford, 1989).
- [38] H. C. Fogedby, *Eur. Phys. J. B* 20, 153 (2001).
- [39] H. C. Fogedby and A. Brandenburg, *Phys. Rev. E* 66, 016604 (2002).
- [40] H. C. Fogedby, *J. Phys.: Condens. Matter* 14, 1557 (2002).
- [41] W. A. Woyczynski, *Burgers-KPZ Turbulence* (Springer-Verlag, New York, 1998).
- [42] A. Scott, *Nonlinear Science* (Oxford University Press, Oxford, 1999), 1st ed.
- [43] G. D. Mahan, *Many-Particle Physics* (Plenum Press, New York, 1990).
- [44] C. W. Gardiner, *Handbook of Stochastic Methods* (Springer-Verlag, New York, 1997).
- [45] H. Risken, *The Fokker-Planck Equation* (Springer-Verlag, Berlin, 1989).
- [46] H. C. Fogedby, *Theoretical Aspects of Mainly Low Dimensional Magnetic Systems* (Springer-Verlag, New York, 1980).
- [47] R. L. Stratonovich, *Topics in the Theory of Random Noise* (Gordon and Breach, New York, 1963).
- [48] S. k. Ma and G. F. Mazonko, *Phys. Rev. B* 11, 4077 (1975).
- [49] U. Deker and F. Haake, *Phys. Rev. A* 11, 2043 (1975).
- [50] L. Landau and E. Lifshitz, *Statistical Physics, Part 2* (Pergamon Press, Oxford, 1980).
- [51] R. Rajaraman, *Solitons and Instantons* (North-Holland, Amsterdam, 1987).

- [52] G. M. Schutz, Phase Transitions and Critical Phenomena, vol. 19 (Academic Press, London, 2000), editors C. Domb and J. L. Lebowitz.
- [53] J. D. Cole, Quart. Appl. Math. 9, 22 (1951).
- [54] E. Hopf, Comm. Pure Appl. Math. 3, 201 (1950).
- [55] H. C. Fogedby, P. Hedegaard, and A. Svane, Physica B 132, 17 (1985).
- [56] L. Landau and E. Lifshitz, Quantum Mechanics (Pergamon Press, Oxford, 1959).
- [57] N. Hatano and D. R. Nelson, Phys. Rev. Lett. 77, 570 (1996).
- [58] N. Hatano and D. R. Nelson, Phys. Rev. E 56, 8651 (1997).
- [59] H. C. Fogedby, J. Hertz, and A. Svane (2002), cond-mat/0212546.
- [60] J. Krug, P. Meakin, and T. Halpin-Healy, Phys. Rev. A 45, 638 (1992).
- [61] S. Machlup and L. Onsager, Phys. Rev. 91, 1512 (1953).
- [62] R. Graham and T. Tel, J. Stat. Phys. 35, 729 (1984).
- [63] M. Prahofer and H. Spohn (2000), math.PR/0105240.
- [64] M. Prahofer and H. Spohn (2000), cond-mat/0101200.
- [65] M. Prahofer and H. Spohn, 279, 342 (2000).

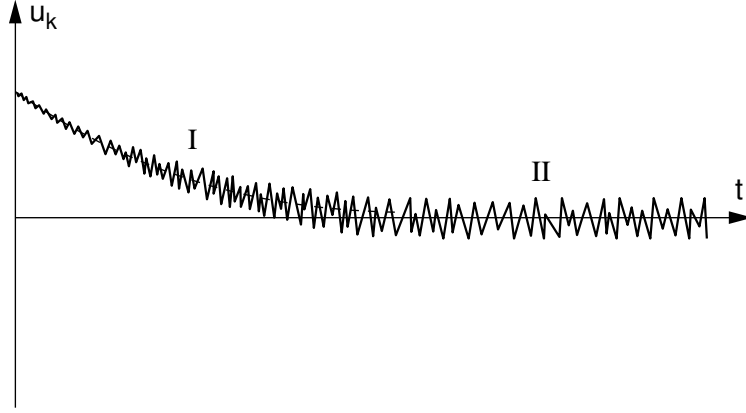


FIG .1: We depict the noisy behavior of a wavenumber component of the slope field, $u_k(t)$, in the Edwards-Wilkinson case for $\gamma = 0$. After a transient period given by $t \sim 1/\lambda_k$ the noise on the same time scale gradually picks up the motion and drives $u_k(t)$ into a stationary noisy state. The transient regime is denoted by I; the stationary regime by II.

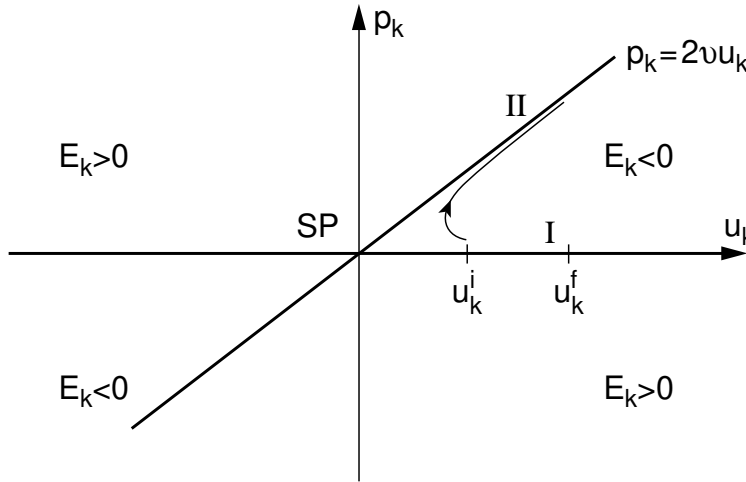


FIG .2: Canonical phase space plot in the linear case for $\gamma = 0$ of a single wavenumber component. The solid lines indicate the transient submanifold $p_k = 0$ (I) and the stationary submanifold $p_k = 2u_k$ (II). The stationary saddle point (SP) is at the origin. For $t \gg 1$ the orbit from u_k^i to u_k^f migrates to the zero-energy manifold. The infinite waiting time at the saddle point corresponds to ergodic behavior.

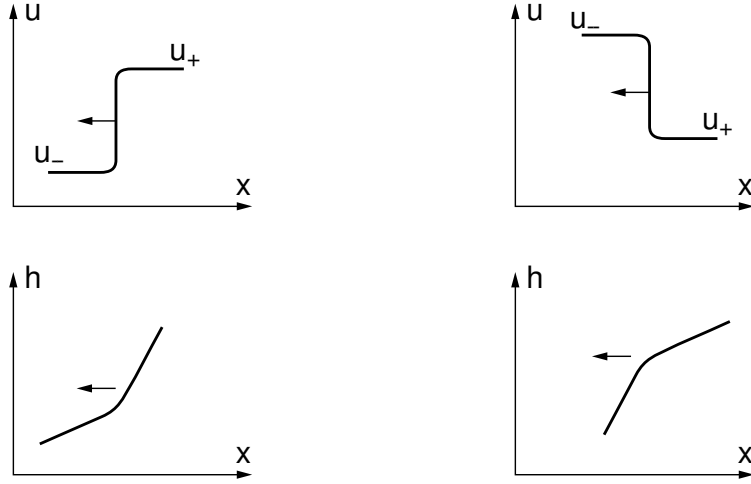


FIG . 3: We depict the right hand and left hand moving solitons forming the "quarks" in the description of a growing interface. We have, moreover, shown the associated height profiles.

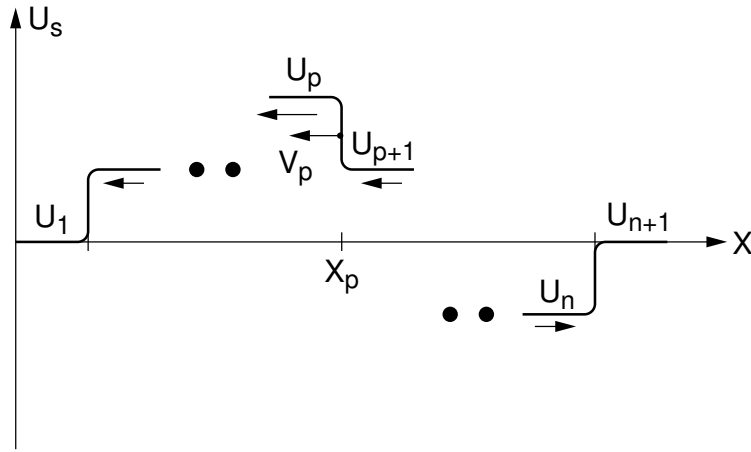


FIG . 4: We depict an n -soliton slope configuration of a growing interface. The p -th soliton moves with velocity $v_p = \frac{1}{2}(u_{p+1} + u_p)$, has boundary values u_+ and u_- , and is centered at x_p . The arrows on the horizontal inter-soliton segments indicate the propagation of linear modes.

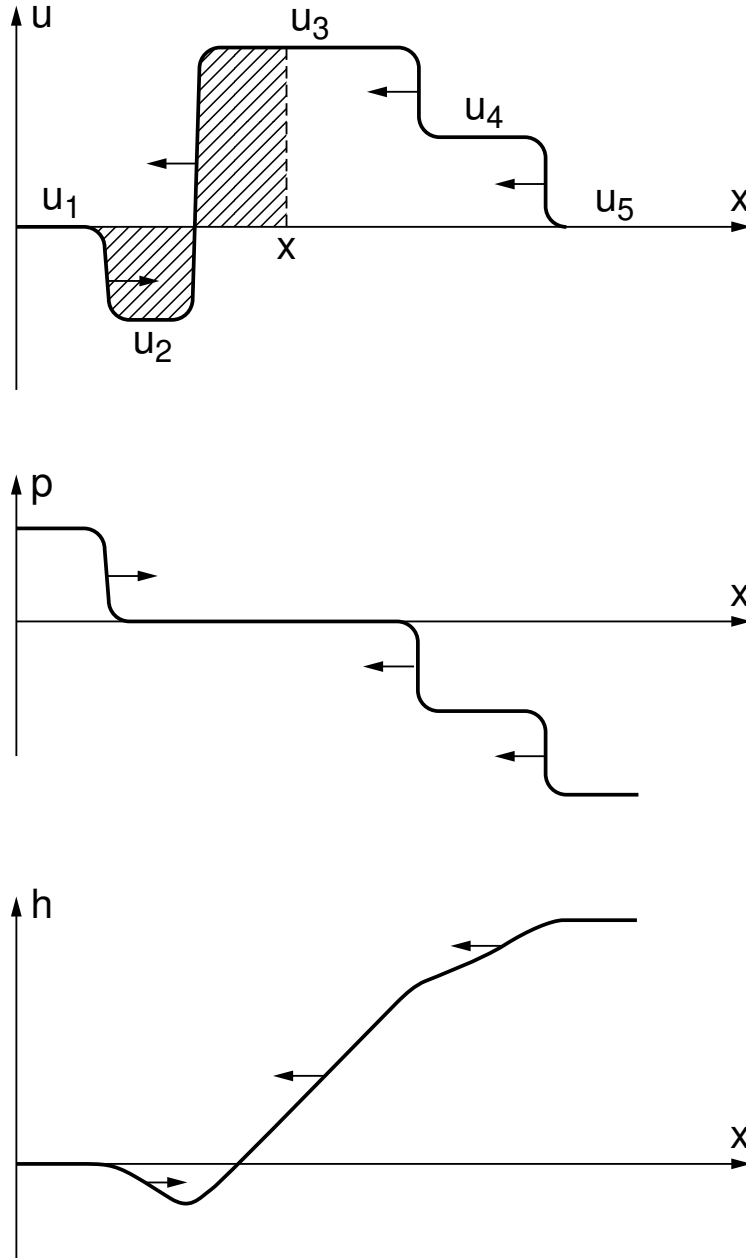


FIG .5: We depict the 4-soliton representation of the slope field u , the noise field p , and the height field h . The shaded area in u , i.e., the integration of u up to the point x equals the height h at x .

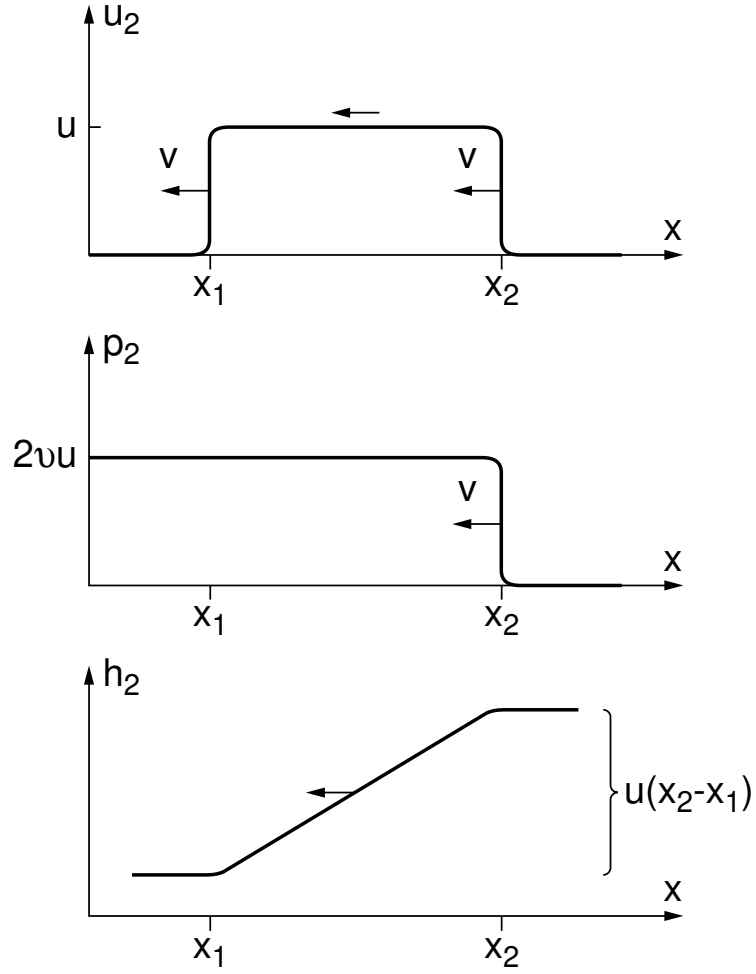


FIG. 6: We depict the slope field u_2 , the associated noise field p_2 , and the resulting height profile h_2 at time $t = 0$ for a two-soliton configuration. The slope configuration has amplitude u , size $\ell = x_2 - x_1$ and propagates with velocity $v = u/2$. The arrow indicates the propagation of the superimposed linear mode with phase velocity $2v$ (discussed in Sec. III).

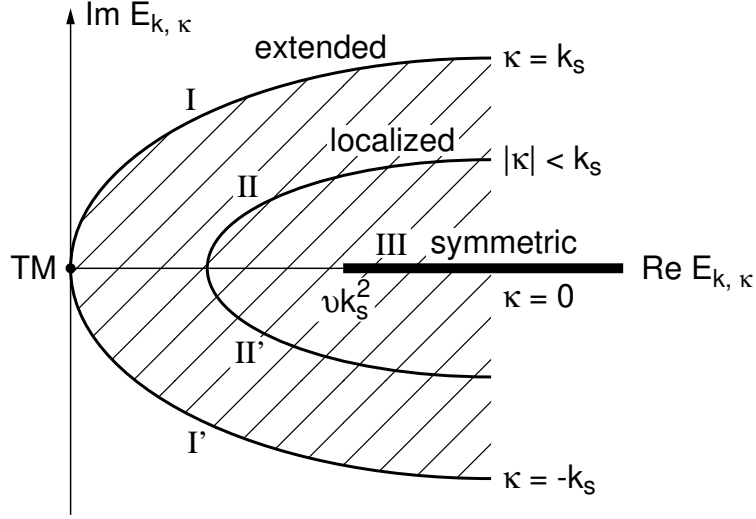


FIG. 7: The complex eigenvalue spectrum for the fluctuating linear modes, $\text{Re } E_{k, \kappa} = (\kappa^2 + k_s^2 - 2)$ and $\text{Im } E_{k, \kappa} = 2\kappa$. The bounding parabola for $\kappa = k_s$ and $\kappa = -k_s$ corresponds to the left and right extended modes propagating towards the soliton center; they are denoted I and I', respectively. The shaded area bounded by the parabola corresponds to localized propagating modes for $\kappa \neq 0$. For $\kappa = 0$ the spectrum is real corresponding to a localized non-propagating symmetric mode. The point TM corresponds to the translation mode.

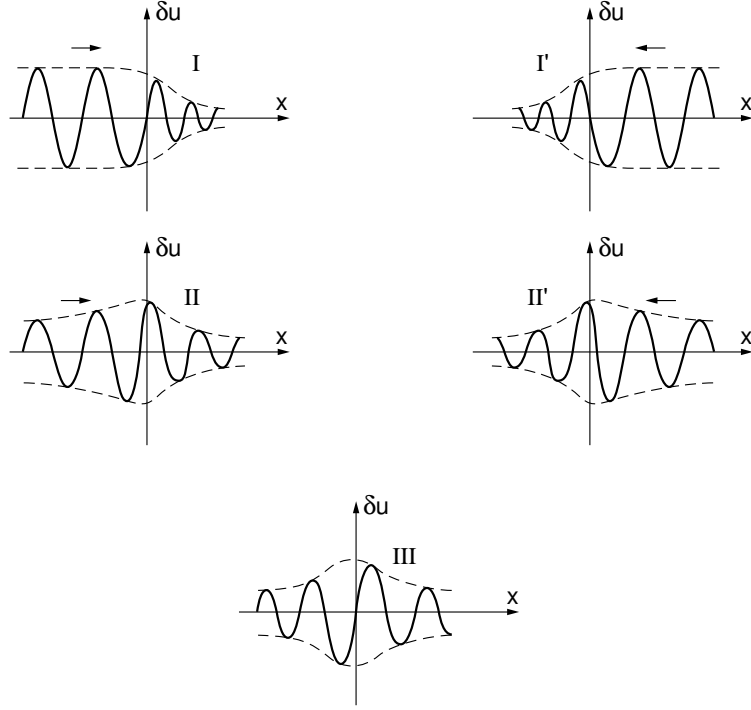


FIG . 8: The fluctuation patterns of the pinned dynamical modes corresponding to the sectors of the eigenvalue spectrum in Fig. 7. The arrows indicate the propagation directions.

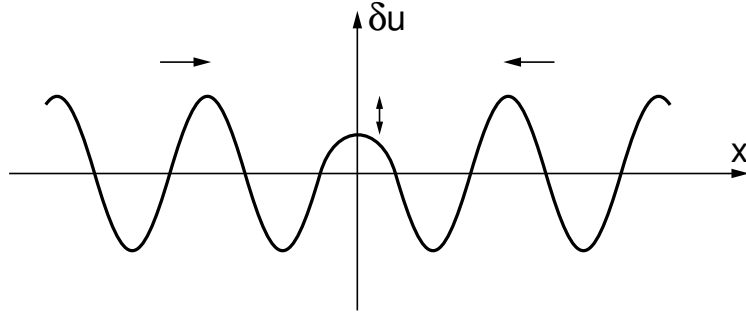


FIG . 9: We depict the extended mode propagating from right and left towards the soliton center which acts like a sink. The center point at $x = 0$ oscillates with frequency $\omega = kv$. The arrows indicate the propagation direction.

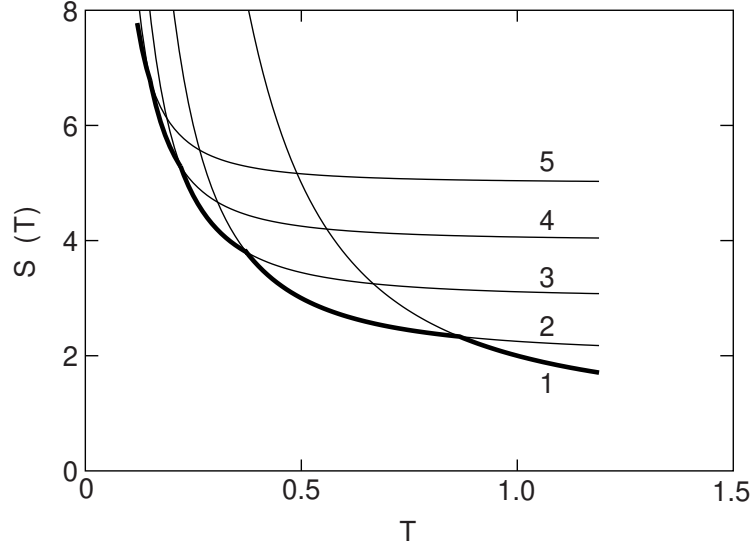


FIG .10: The action given by Eq. (4.11) is plotted as a function of T for transition pathways involving up to $n = 5$ soliton pairs. The lowest action and thus the most probable transition is associated with an increasing number of soliton pairs at shorter times, indicated by the heavy limiting curve. The curves are plotted in arbitrary units.

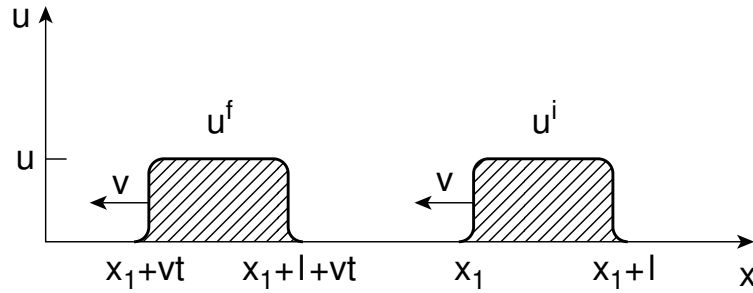


FIG .11: We depict the two-soliton configuration in the limit $l \rightarrow 0$ contributing to the slope correlations hu_i . The initial pair u^i propagates to the final configuration u^f in time t with velocity $v = u/2$.

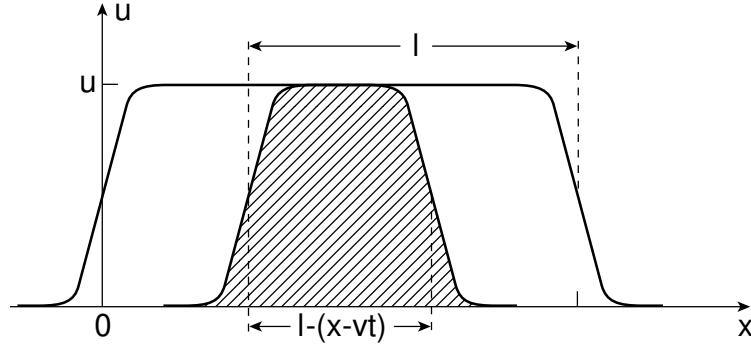


FIG. 12: The two-soliton configuration of size $l = |x_1 - x_2|$ and amplitude u . The shaded overlap area of size $2l - x$ yields a contribution to the slope correlation function.

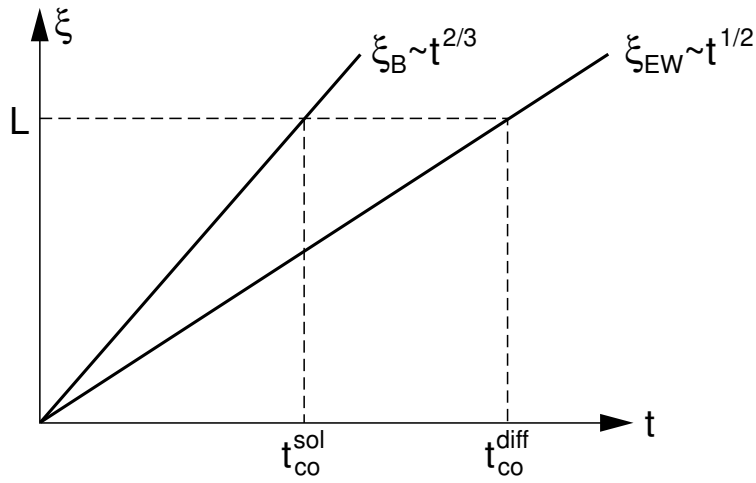


FIG. 13: The correlation lengths $\xi_{EW}(t) = (\nu t)^{1/2}$ and $\xi_B(t) = (\nu t)^{1/3} (\nu t)^{2/3}$ as functions of t . For a finite system of size L the correlation lengths define the crossover times $t_{co}^{diff} / L^2 = \nu$ and $t_{co}^{sol} / \nu^{1/3} (\nu t)^{1/2} L^{3/2}$, determining the transition from transient to stationary growth.

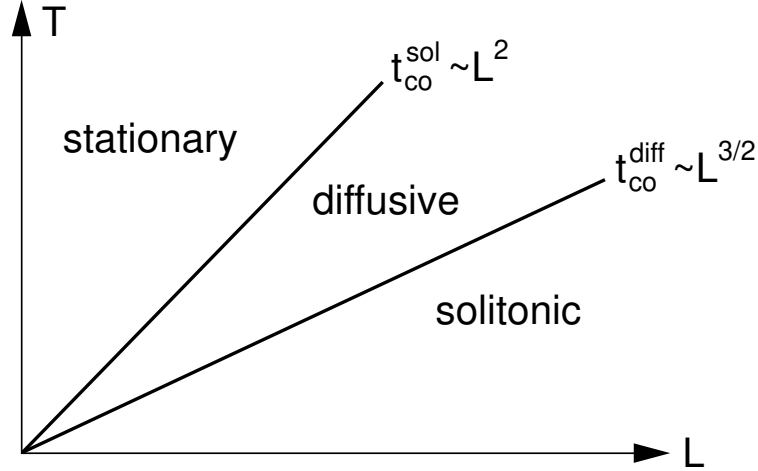


FIG. 14: In the early time regime for $T < t_{co}^{sol}$ the distribution is dominated by solitons. In the intermediate time regime for $t_{co}^{diff} < T < t_{co}^{sol}$ the solitons become suppressed and are replaced by the diffusive modes. Finally, for $T > t_{co}^{diff}$ the diffusive modes also die out and we approach the stationary distribution.

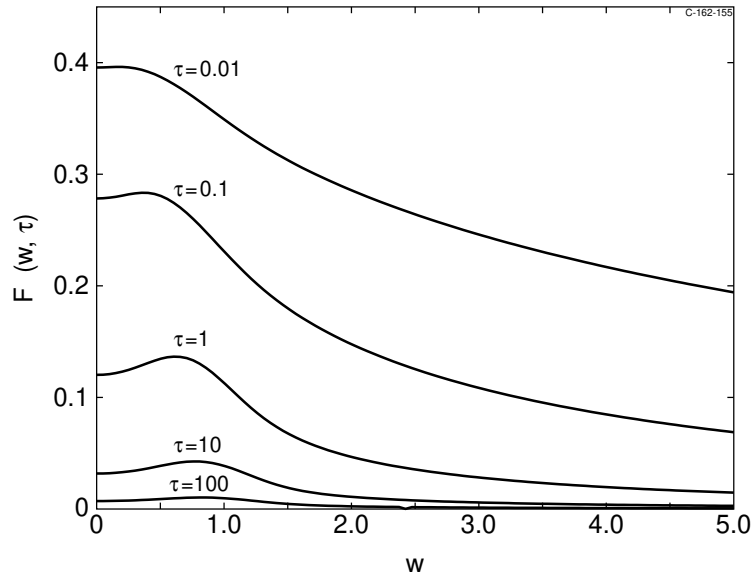


FIG. 15: Plot of the scaling function $F(w; \tau)$ as a function of the scaling variable $w = x / x = t^{2/3}$ for a range of values of $\tau = t / t_{co} = L^{3/2}$.